MicroRNA-199a-3p and MicroRNA-199a-5p Take Part to a Redundant Network of Regulation of the NOS (NO Synthase)/NO Pathway in the Endothelium

Virginie Joris, Elvira Leon Gomez, Lisa Menchi, Irina Lobysheva, Vittoria Di Mauro, Hrag Esfahani, Gianluigi Condorelli, Jean-Luc Balligand, Daniele Catalucci, Chantal Dessy

Objective—Members of the microRNA (miR)-199a gene, namely miR-199a-5p and miR-199a-3p, have been recently identified as potential regulators of cardiac homeostasis. Also, upregulation of miR-199a expression in cardiomyocytes was reported to influence endothelial cells. Whether miR-199a is expressed by endothelial cells and, if so, whether it directly regulates endothelial function remains unknown. We investigate the implication of miR-199a products on endothelial function by focusing on the NOS (nitric oxide synthase)/NO pathway.

Approach and Results—Bovine aortic endothelial cells were transfected with specific miRNA inhibitors (locked-nucleic acids), and potential molecular targets identified with prediction algorithms were evaluated by Western blot or immunofluorescence. Ex vivo experiments were performed with mice treated with antagomiRs targeting miR-199a-3p or -5p. Isolated vessels and blood were used for electron paramagnetic resonance or myograph experiments. eNOS (endothelial NO synthase) activity (through phosphorylations Ser1177/Thr495) is increased by miR-199a-3p/-5p inhibition through an upregulation of the PI3K (phosphoinositide 3-kinase)/Akt (protein kinase B) and calcineurin pathways. SOD1 (superoxide dismutase 1) and PRDX1 (peroxiredoxin 1) upregulation was also observed in locked-nucleic acid–treated cells. Moreover, miR-199a-5p controls angiogenesis and VEGFA (vascular endothelial growth factor A) production and upregulation of NO-dependent relaxation were observed in vessels from antagomiR-treated mice. This was correlated with increased circulated hemoglobin-NO levels and decreased superoxide production. Angiotensin infusion for 2 weeks also revealed an upregulation of miR-199a-3p/-5p in vascular tissues.

Conclusions—Our study reveals that miR-199a-3p and miR-199a-5p participate in a redundant network of regulation of the NOS/NO pathway in the endothelium. We highlighted that inhibition of miR-199a-3p and -5p independently increases NO bioavailability by promoting eNOS activity and reducing its degradation, thereby supporting VEGF-induced endothelial tubulogenesis and modulating vessel contractile tone. **(*Arterioscler Thromb Vasc Biol*. 2018;38:00-00. DOI: 10.1161/ATVBAHA.118.311145.)**

Key Words: endothelial cells ■ endothelium ■ microRNA ■ nitric oxide ■ oxidative stress

Endothelial dysfunction characterized by reduced NO (nitric oxide) bioavailability is commonly recognized as a cause and consequence of most cardiovascular diseases.[1] In the endothelium, NO production mostly arises from the conversion of L-arginine to equimolar amounts of citrulline and NO, catalyzed by eNOS (endothelial NO synthase). In response to agonists or fluid shear stress, eNOS activation requires a cascade of events that start with changes in cytosolic Ca^{2+}, translocation of the enzyme from caveolar microdomains to the oxygen-rich cytosol, followed by substrate and cofactors interactions.[2–5] An additional layer of regulation results from post-translational modifications of eNOS, including activating/inactivating phosphorylation, glycosylation, glutathionylation, nitrosylation, and acetylation.[2,6]

Decreased availability of the substrate L-arginine contributes to NO deficiency and endothelial dysfunction. This is observed when the breakdown of L-arginine by arginase is accelerated as reported in the context of aging, diabetes mellitus, and hypertension. In these conditions, elevated serum levels of asymmetric dimethyl arginine (ADMA), the endogenous negative competitor of arginine, also participate in the reduction of NO production.[7] Oxidative stress is another common denominator to many cardiovascular diseases characterized by endothelial dysfunction. In diabetes mellitus, atherosclerosis, or hypertension, generation of superoxide anions

Received on: December 22, 2017; final version accepted on: June 20, 2018.

From the Pole of Pharmacology and Therapeutics, Experimental and Clinical Research Institute (IREC), Université catholique de Louvain, Brussels, Belgium (V.J., E.L.G., L.M., H.E., J.-L.B., C.D.); Humanitas University, Rozzano (Milan), Italy (V.D.M., G.C.); Humanitas#8232, Clinical and Research Center, Rozzano (Milan), Italy (V.D.M., G.C., D.C.); and Institute of Genetics and Biomedical Research, Milan Unit, National Research Council, Italy (V.D.M., G.C., D.C.).

The online-only Data Supplement is available with this article at http://atvb.ahajournals.org/lookup/suppl/doi:10.1161/ATVBAHA.118.311145/-/DC1.

Correspondence to Chantal Dessy, Pole of Pharmacology and Therapeutics, Experimental and Clinical Research Institute (IREC), Université catholique de Louvain, Ave Mounier 52 1200, Brussels, Belgium. Email chantal.dessy@uclouvain.be

Nonstandard Abbreviations and Acronyms

ADMA	asymmetric dimethyl arginine
Akt	protein kinase b
BAEC	bovine aortic endothelial cells
Cav	caveolin
DDAH	dimethylarginine dimethylaminohydrolase
DETC	diethyldithiocarbamate
DNM	dynamin
eNOS	endothelial NO synthase
EPR	electron paramagnetic resonance
HbNO	hemoglobin-NO
LNA	locked-nucleic acid
miRNA/miR	microRNA
mTOR	mammalian target of rapamycin
NO	nitric oxide
PDK	pyruvate dehydrogenase kinase
PI3K	phosphoinositide 3-kinase
PRDX	peroxiredoxin
PRMT	protein arginine N-methyltransferase
RT	room temperature
SOD	superoxide dismutase
VEGFA	vascular endothelial growth factor A

(also produced by uncoupled NOS) leads to the formation of (deleterious) peroxynitrite thereby reducing the abundance of bioactive NO.[8,9] Although eNOS expression is only subject to modest degrees of regulation in physiological conditions, transcriptional and post-transcriptional modes of eNOS regulation are frequently described in pathological states,[10] including heart failure,[11] atherosclerosis,[10,12] diabetes mellitus, and hypercholesterolemia.[13,14]

Among post-transcriptional regulations, epigenetic mechanisms are less well studied. MicroRNAs (miRNAs/miRs) are highly conserved, small noncoding RNAs which negatively regulate gene expression. The miRNA-199a gene, comprising miR-199a-3p and -199a-5p, was originally described in cancer cells because of its capacity to regulate proliferation[15] and angiogenesis.[16] In the past years, interest arose in the cardiovascular field when van Rooij et al reported that miR-199a takes part in a miRNA signature associated with cardiac hypertrophy and heart failure.[17–19] Other investigators showed that cardiomyocyte-specific overexpression of miR-199a was sufficient to impair cardiomyocyte autophagy and thereby induce cardiac hypertrophy through mTOR (mammalian target of rapamycin) activation.[20] Paradoxically, another study using myocyte-specific miR-199a-sponge documented that a 20% to 30% decrease in endogenous miR-199a-5p levels leads to physiological cardiac hypertrophy through the upregulation of metabolism-related gene expression.[21]

Interestingly, tissue profiling analysis has revealed that miR-199a is highly expressed in rat lung and cardiac tissues.[22] In the heart, miR-199a was predominantly, but not exclusively, expressed in cardiomyocytes. Also, changes in miR-199a expression in cardiomyocytes were reported to influence neighboring cells. In particular, an increase in ADMA levels in the culture supernatant of pre-miR-199a-exposed cardiomyocytes actually lowered NO bioavailability in rat cardiac endothelial cells.[23] Although the above studies suggested that miR-199a may play critical roles in various tissues, including blood vessels, whether they are expressed by endothelial cells and if so, whether they regulate endothelial function are largely unexplored. Here, we have used bioinformatic algorithms to predict potential targets of miR-199a in endothelial cells and validated several of them through the dissection of the in vitro and in vivo effects of miRNAs 199a-targeting locked-nucleic acid (LNA) and antagomiR, respectively, on eNOS activity.

Materials and Methods

The authors declare that all supporting data are available within the article (and in the online-only Data Supplement).

Cell Culture and LNA Transfection

Bovine aortic endothelial cells (BAEC) were cultured on 0.2% gelatin-coated 12-well plates using DMEM (Gibco) supplemented with 10% FBS and 100U penicillin/100 µg streptomycin. Endothelial cells were plated into 12-well culture plates and transfected with 40 nM LNA targeting miR 199a-3p (Exiqon 4100888-001), -5p (Exiqon 4101096-001), mimics (Qiagen YM00472279 and YM00471589), or scramble sequence (Exiqon 199006-001) overnight using DNA Transfection Reagent (Biotool) in Opti-Mem diluted in DMEM supplemented with 10% FBS without antibiotics. Transfection was stopped by replacing transfection medium with complete culture medium (DMEM+FBS 10%+antibiotics). For the immunoblotting, cells were collected 48 or 72 hours after transfection in RIPA lysis buffer (Tris HCl 50 mmol/L, NaCl 150 mmol/L, EDTA 1 mmol/L, 0.1% SDS, 0.5% sodium deoxycholate, Triton-100× 10%) containing a protease inhibitor cocktail (Sigma) and a phosphatase inhibitor (Roche). Transfection efficiency was characterized by studying the modulation of direct targets of miR-199a-3p, -5p in endothelial cells after inhibition of these miRNAs.

Pharmacological Treatments

For the PI3K (phosphoinositide 3-kinase)/Akt (protein kinase B) inhibition experiments, LY294002 treatment (LY, 20 µM; Millipore) was initiated 1 day before LNA transfection and maintained up to the harvesting of the cells. For inhibition of VEGFA (vascular endothelial growth factor A), Bevacizumab (2 µM; Roche) was used during LNA transfection and maintained up to harvesting. Forty-eight hours after transfection, cells were collected in RIPA lysis buffer to perform immunoblotting.

LNA and Akt1 siRNA Cotransfection

To study the implication of Akt1 in the pathway modulated by miRNA inhibition, we have proceeded in 2 steps. Endothelial cells were plated into 12-well culture plates and transfected during 5 hours with 50 nM of siRNA directed against Akt1 (Riboxx) using Lipofectamine RNAimax (Invitrogen) in Opti-Mem diluted in DMEM supplemented with 10% FBS. Transfection was stopped by adding complete culture medium (DMEM+FBS 10%+antibiotics). After overnight recovery, cells were transfected with 40 nM of each LNA or control sequence using Lipofectamine RNAimax in Opti-Mem diluted in DMEM supplemented with 10% FBS. Once again, transfection was stopped by adding complete culture medium (DMEM+FBS 10%+antibiotics). Cells were collected 48 hours after the second transfection in RIPA lysis buffer.

miRNA Extraction

Endothelial cells were suspended in homogenisation buffer provided by Promega in the Maxwell RSC miRNA Tissue Kit (ref AS1460) and added with thioglycerol (20 µl/1 mL). Heart and vessel tissues

were crushed in homogenisation buffer added with thioglycerol, and plasmas were just added with thioglycerol. Samples were processed following the manufacturer's instructions. In brief, lysis buffer and proteinase K were added to the samples and mixed by vortexing. Samples were incubated at room temperature (RT) during 10 minutes and loaded in cartridges provided in the kit. Cartridge was previously prepared by adding 10 µl of DNAse 1, excepted for samples where miR inhibition by LNA was measured. Samples were processed using Maxwell RSC Instrument (Promega) for miRNA extraction and eluted in nuclease-free water.

miRNA Reverse Transcription and Quantitative PCR

Reverse transcription and quantitative polymerase chain reaction (PCR) for miR were performed following the protocol A for individual assays provided with miRCURY LNA Universal RT microRNA PCR kits (Exiqon 203301–203351). First-strand cDNA synthesis was performed with 2 µl of RNA sample adjusted to a concentration of 5 ng/µL. RT mix containing reaction buffer and enzyme mix was added to the samples and incubated at 42°C during 1 hour followed by a step of heat-inactivation at 95°C for 5 minutes. Regarding the quantitative PCR, samples were diluted following manufacturer's recommendations, and 4 µl were loaded in 96-well PCR plates. PCR master mix and PCR primers set were added, and PCR was performed in iQ5 cycler Biorad machine following the kit protocol. Primers used were the following miR-199a-3p (Exiqon 204536), miR-199a-5p (Exiqon 204494), U6 (Exiqon 203907), and miR-let-7i-5p (Exiqon 204394), the latter was used for plasma and vessels following the recommendations of the manufacturer.

Western Blot

Endothelial cells and tissues were suspended in RIPA lysis buffer. A Bicinchoninic Acid Protein Assay Kit (Pierce) was used to determine the protein concentration of each sample according to the manufacturer's protocol. Ten µg of proteins were loaded per Western blot well, and the migration was performed in migration buffer (Tris-EDTA, SDS, glycine) under a voltage of 120 V. After migration, proteins were transferred on a nitrocellulose membrane with constant amperage of 350 mA for 1 hour 30 minutes (transfer buffer: Tris-base, glycine, SDS, methanol). The membranes were then incubated in a blockage solution consisting in TBS-Tween 0.1% BSA 5% for 1 hour at RT. For the immuno-detection of the targeted proteins, primary antibodies were incubated overnight at 4°C in TBS-Tween/BSA 5%. Primary antibodies are the following: anti-phosphoSer1177eNOS (1 µl/mL; Cell Signaling, 9571), anti-phosphoThr308Akt (1 µl/mL; Cell Signaling, 2965), anti-Akt (1µl/mL; Cell Signaling, 9272) anti-Akt1 (1 µl/mL; Cell Signaling, 2938), anti-phosphoTh495eNOS (0.5 µg/mL; BD transduction, 612706), anti-calcineurin (1 µg/mL; Millipore, 07–1491), anti-SOD1 (superoxide dismutase 1; 1 µg/mL; Abcam, ab13498), anti-Cav1 (caveolin-1; 0.05 µg/mL; BD transduction, 610407), anti-Hsp90 (0.25 µg/mL; BD transduction, 610419), anti-DDAH1 (dimethylarginine dimethylaminohydrolase; 0.5 µg/mL; Abcam, ab2231), anti-PRMT1 (protein arginine N-methyltransferase; 2.5 µg/mL; Abcam, ab12189), anti-PDK1 (pyruvate dehydrogenase kinase; 2 µg/mL; Gentaur, KAP-PK112), anti-βactin (0.02 µl/mL; Sigma, A5441), and anti-VEGFA (1 µg/mL; Abcam, ab46154); this last antibody recognizes all the splicing forms of VEGFA. Membranes were washed in TBS-Tween and incubated with the peroxidase-conjugated secondary antibody for 1 hour at RT and developed by enhanced chemiluminescence (ECL, Amersham) on CL-Xposure film (Thermo Scientific). Films were scanned, and protein bands were quantified by densitometry using ImageJ software (National Institutes of Health). Levels of all proteins of interest were normalized to β-actin level. The levels of phosphorylated proteins were normalized to the level of total proteins.

NO Measurement on Cells

Electron paramagnetic resonance (EPR) spectroscopy was used to detect NO production in BAECs after formation of the paramagnetic adduct Fe(II)NO (diethyldithiocarbamate)$_2$ in reaction of NO with the spin trap [Fe(II)(diethyldithiocarbamate)$_2$] as previously described.[24] In brief, cells transfected with LNA were treated with or without L-nitroarginine methyl ester (2.5 mmol/L) for 1 hour and incubated for 30 minutes at 37°C with KREBS buffer (NaCl 99 mmol/L, KCl 4.69 mmol/L, KH_2PO_4 1.03 mmol/L, $MgSO_4$ 1.2 mmol/L, $NaHCO_3$ 25 mmol/L, glucose 5 mmol/L, HEPES 20 mmol/L, and $CaCl_2$ 2 mmol/L) containing 0.2% BSA. Cells were then treated for 45 minutes at 37°C with 0.5 mmol/L of [diethyldithiocarbamate]2-Fe(II) colloid complex, scrubbed, and frozen in calibrated tubes. The EPR signals were recorded with following EPR parameters: microwave power, 20 mW; modulation amplitude 5G; time constant, 80 ms; 7 scans; 77 K, and normalized per µg of proteins.

Immunofluorescence

BAEC cells were fixed in paraformaldehyde 4% for 10 minutes at RT, washed in PBS, and blocked for 1 hour at RT in PBS containing 0.1% saponin and 5% BSA. PRDX1 (peroxiredoxin 1) was detected by incubating the fixed cells with anti-PRDX1 rabbit primary polyclonal antibody (5 µg/mL; Abcam, ab15571) in PBS/saponin 0.1%/BSA 1% at 4°C overnight, followed by incubation with Alexa Fluor 488-conjugated goat anti-rabbit (6 µg/mL; Life's technologies) for 1 hour at 37°C. Cells were incubated with Dapi nuclear stainer (1:10 000 in PBS) for 5 minutes at RT and mounted with Dako fluorescent Medium (Dako). Negative controls were performed by incubation with the secondary antibody only.

Dihydroethidium Staining

Dihydroethidium is able to permeate cells. In the presence of superoxide anion, it is oxidized to 2-hydroxyethidium and ethidium, which are trapped by intercalation with DNA resulting in bright red fluorescence. In brief, cells were cultured in 12-well vessels on gelatin-coated cover glasses and transfected with LNA, as described above. After 48 hours, cells were washed with PBS and incubated in the presence of dihydroethidium (10 µM) for 1 hour at 37°C. Cells were incubated with Hoechst nuclear stainer (1:10 000 in PBS) for 5 minutes at RT and mounted with Dako fluorescent Medium (Dako). Nuclear staining of dihydroethidium is directly analyzed using Axioskop 40 microscopy system.

ADMA Measurement

To assess ADMA level in culture media, ADMA high sensitive ELISA kit from DLD diagnostika GMBH (EA209/96) was used following the manufacturer recommendations. In brief, ADMA in the samples is acylated and competes with ADMA bound in the microtiter plate for a fixed number of rabbit anti-ADMA antiserum binding sites. The absorbance is read at 450 nM with spectrophotometer and is inversely proportional to the ADMA concentration of the sample.

Angiogenesis Test

BAEC were transfected overnight with LNA or scramble sequence on 0.2% gelatin-coated plates. After transfection, cells were trypsinized, counted, and mixed in equal volume with growth factor–reduced Matrigel (≈10 mg/mL proteins). Each mixture was put in culture in 12-well plate. After polymerization of the Matrigel for 1 hour at 37°C, each well containing mixture with cells was covered with 500 µl of complete medium. Each condition was performed in duplicate. After 48 and 72 hours, cells underwent migration and alignment to form tubes.

Luciferase Assay

A 3' UTR fragment of the VEGFA, calcineurin, and SOD1 mRNAs were subcloned by using In-Fusion HD Cloning Kits (Clonotech) according to manufacturer's instruction, into the pmiRGlo Dual-Luciferase vector (Promega) immediately downstream of 3´ of the firefly luciferase gene (luc2).

The miR-199a/a* mature sequence was cloned into the pcDNA6.2-GW/EmGFP-miR vector according to the manufacturer's

protocol (Thermo Fisher Scientific). 2.5×105 HeK-293T cells were transfected with pmiRGlo-3'UTR and pcDNA6.2-GW/EmGFP-miR-199a/a* (miR-199a-5p/-3p) plasmids. Forty-eight hours post-transfection, cells were lysed, and luciferase activity was measured using the Nano-Glo Dual-Luciferase Reporter (NanoDLR) Assay System as described by the manufacturer (Promega). To confirm specific targeting of the 3'UTR of target genes by miR-199a/a*, site-specific mutagenesis at the predicted sites were obtained by using the QuikChange Site-Directed Mutagenesis Kit according to the manufacturer's instructions (Agilent technologies). Mutated constructs were then tested in luciferase assays, and the rescue of chemiluminescent signal in the presence of miR-199a/a* identified real targeting sites. Moreover, alignments between human and bovine sequences were performed using clustalW and assessed that within the calcineurin gene, the putative binding sites for both miR-199a family members are conserved between *Homo Sapiens* and *Bos Taurus*. VEGFA gene has only the region containing the putative binding site for miR-199a-5p, which is conserved between the 2 species. Concerning SOD1 gene, conservation of miR-199a-3p and -5p sites is almost identical except for few nucleotides between *Homo Sapiens* and *Bos Taurus*.

Animals and Treatments

All experimental procedures and protocols were approved by the local Ethics Committee (Comité d'Ethique pour l'Expérimentation animale), Secteur des Sciences de la Santé, Université Catholique de Louvain, according to National Care Regulation and Directive 2010/63/EU of European Parliament and of the Council. Only male mice were used in this study to avoid confounding effects. Indeed, estrogens are well-characterized modulators of endothelial function through regulation of the NOS/NO pathway.

Seven-week-old C57Bl6 male mice (30 animals) were injected in caudal vein 3 days in a row with a specific antagomiR (Fidelity systems, 75 mg/kg per day) directed against miR-199a-3p and -5p specifically, a scramble sequence or saline solution.[25–27] These injections were performed each day by the same experimented technician. Mice were then housed 1 per cage in a 12/12-hour night and day cycle for 30 days, and their behavior was checked every day. At the day of the euthanization, blood and vessels were collected; the arteries were mounted on a wire myograph to evaluate the endothelium-dependent response, some vessels samples were frozen for further analysis (Western blotting as described above). Blood samples were used for assessment of NO and superoxide anion rates by EPR or plasma isolated for miR profiling.

Twelve-week-old C57Bl6/J male mice (12 animals) were treated with continuous infusion of angiotensin II (2 mg/kg per day) or saline solution during 14 days using osmotic minipumps (Alzet 2002) subcutaneously implanted between the scapulae in anesthetized mice with Isoflurane, as described in the literature.[28] Mice were housed 1 per cage after the implantation of the minipumps, and their wellbeing was checked every day. After 14 days, terminal anesthesia was performed by intraperitoneal injection of ketamine (100 mg/mL) and xylazine (20 mg/mL), mice were weighed, blood, heart, and vessels were collected and frozen in liquid nitrogen for further miR profiling.

Bias and Randomization

All mice were cared for equally in an unbiased fashion by animal technicians and investigators. Mice were randomly allocated into 4 groups (Figure 6) or 2 groups (Figure IX in the online-only Data Supplement). Although the mouse groups were not blinded, the people involved in functional studies on vessel relaxation, in hemoglobin-NO (HbNO) dosage, osmotic pump surgical implantation, and quantitative PCR were different, and data were never shared between them up to article writing. In addition, HbNO dosage and osmotic pump-related surgery were performed by platform logisticians and quantitative PCR by Masters students who were not aware of the nature of the study. Finally, we took care of adding a saline solution condition besides the antagomir scramble control to exclude any bias related to the mouse injection, including the stress associated with mouse handling. For the same reasons, minipumps loaded with saline solution were implanted to be used as the most appropriate control of angiotensin-loaded pumps.

NO Measurement in Venous Blood

NO bioavailability was assayed as the concentration of circulating hemoglobin nitrosylated at heme-FeII (HbNO) in vivo. Whole venous blood of male C57Bl6 mice treated or not with antagomiRs against miR-199a-3p, -5p or scrambled antagomiR was collected and frozen immediately in calibrated tubes as previously described.[29] The EPR spectra were recorded by a Bruker spectrometer (AMXmicro, X-band; microwave frequency 9.35 GHz, modulation frequency 100 kHz) with following setting: microwave power, 20 mW; modulation amplitude, 0.7 mT; 5 scans, at 77 K using a finger dewar. The level of HbNO was quantified from hyperfine structure (gz=2.011; Az=16.8G) of the EPR signal after digital subtraction of a signal of protein-centered free radicals (g=2.005; linewidth≈19G) using Bruker software, Xenon. Samples were normalized by volume.

Anion Superoxide Measurement in Aortic Rings

Superoxide anion production was assayed quantitatively by EPR in isolated aortic rings using ROS-sensitive spin probe at 1 mmol/L (1-hydroxy-3-methoxycarbonyl-2,2,5,5-tetramethylpyrrolidine, CM-H; Alexis Biochemichal, Inc) in situ, as previously described.[30] In brief, aortic rings were preincubated in KREBS-DTPA-Hepes buffer (0.1 mmol/L DTPA, 20 mmol/L HEPES, pH 7.5) in presence or not of SOD (100U/mL). Then the aortic rings were inserted in capillaries and the kinetics of the CM·EPR signal formation was recorded on-line in capillary interposed into the cavity of the EPR spectrometer during 10 to 15 minutes at 37°C (10 scans) using the X-band EPR spectrometer MS400, Magnettech (microwave frequency, 100 kHz; microwave power, 20 mW; modulation amplitude, 0.1 mT). The rate of the CM· radical formation was calculated as a slope of linearized kinetic curve. Results were normalized by the length of aortic ring. SOD-sensitive signal was accepted as superoxide anion formation.

Myograph Experiments

Thoracic aortic arteries were mounted in a wire myograph. NO-mediated relaxation was measured as previously described.[31,32] In brief, 2 40 µm wires were threaded into the lumen of the vessel segments and incubated in a bath continuously perfused with physiological solution, gassed, and maintained at 37°C. Aorta from antagomiR-treated or control mice was contracted with a high-KCl solution (to prevent implication of EDHF) in the presence of indomethacin (10 µmol/L), a Cox2 (cyclooxygenase-2) inhibitor, and exposed to an increased concentration of acetylcholine.

Statistical Analyses

All experiments were reproduced at least 3×. All data are expressed as the mean±SEM. Shapiro-Wilk normality test and Bartlett or Levene equal variance tests were performed, and statistically significant differences were determined using a 2-way ANOVA or 1-way ANOVA followed by Tukey-Kramer post hoc ANOVA test or by using a Kruskal-Wallis test for nonparametric data. $P<0.05$ was considered statistically significant.

Results

miR-199a-3p and miR-199a-5p Are Expressed in Endothelial Cells

As a preamble to this study, we first evaluated the expression of the mature miR-199a arising from both arms of the precursor miR-199a, respectively miR-199a-3p (3'arm) and miR-199a-5p (5' arm) in human and BAEC. Of note, sequences

of human and bovine miR-199a are strictly identical. Both mature miRNAs were detected in significant and similar amounts in endothelial cells (PCR threshold cycle values for miR-199a-5p and -3p in BAEC: Ct 27.4 and 27.5 and in human aortic endothelial cells: Ct 26.3 and Ct 26.4, respectively). We used bioinformatic algorithms (target scan, Pictar, miRNA.org) to predict potential targets of miR-199a-3p and -5p in endothelial cells, in particular in the eNOS/NO pathway (Table). Although eNOS gene per se was not identified as a theoretical target for either miR-199a, matching sequences were identified in a series of genes coding for proteins related to the NO pathway (see below). Matching between miR-199a-3p or miR-199a-5p and some of the predicted targets were verified using luciferase-based reporter assays. As highlighted in Figure I in the online-only Data Supplement, both miR-199a-3p and miR-199a-5p target the 3'UTR region of *VEGFA, Calcineurin,* and *SOD1* mRNA.

NO Production Is Increased After Repression of miR-199a-3p or miR-199a-5p in Endothelial Cells

Transfection of LNA directed against either arm of miR-199a was effective in reducing the expression of the targeted miR as measured 48 or 72 hours after transfection (Figure IIA and IIB in the online-only Data Supplement). LNA-based repression of miR-199a-3p or miR-199a-5p practically doubled basal NO production in BAECs (Figure 1). Treatment of BAECs with the nonselective NOS inhibitor L-nitroarginine methyl ester reduced NO levels to baseline amounts, indicating that miR-199a-3p or -5p blockade somehow led to an increase in NOS synthase(s) activity or in bioavailable NO. The expression of eNOS (the predominant NOS isoform expressed in endothelial cells) was not significantly altered by repression of miR-199a-3p or -5p (see total eNOS in Figure 2A). Similarly, expression of Cav1 and hsp90, 2 critical eNOS regulators in endothelial cells, remained unaltered after LNA treatments (Figure III in the online-only Data Supplement). Also, neither the presence (in culture media) of ADMA, the endogenous competitive substrate for eNOS, nor the expression of its production/degradation enzymes in endothelial cells, namely DDAH1 and PRMT1 (the latter being a theoretical potential miR-199a target [Table]), were affected by either LNA treatments (Figure IVA–IVC in the online-only Data Supplement).

eNOS Phosphorylation on Ser1177 is Modulated by miR-199a-3p and miR-199a-5p Repression Through the PI3K/Akt Pathway

Post-translational modifications of eNOS include changes in its phosphorylation state. We found that miR-199a-3p and

Table. miRSVR, TargetScan, and Pictar Scores for Indicated Target mRNA

	miR	miRSVR	TargetScan	Pictar	miRSVR Mouse
eNOS	miR-199a-3p	n.i.	n.i.	n.i.	n.i.
	miR-199a-5p	n.i.	n.i.	n.i.	n.i.
Akt1	miR-199a-3p	n.i.	n.i.	n.i.	–0.0011
	miR-199a-5p	n.i.	n.i.	n.i.	n.i.
Calcineurin	miR-199a-3p	–0.03	–0.24	1.78	–0.0305
	miR-199a-5p	n.i.	n.i.	3	–0.0366
PDK1	miR-199a-3p	n.i.	n.i.	n.i.	–0.1428
	miR-199a-5p	n.i.	n.i.	n.i.	–0.1813
CAV1	miR-199a-3p	n.i.	n.i.	n.i.	–0.0497
	miR-199a-5p	–0.8069	–0.68	3.88	–0.47
HSP90	miR-199a-3p	n.i.	n.i.	n.i.	–0.0273
	miR-199a-5p	n.i.	n.i.	n.i.	n.i.
SOD1	miR-199a-3p	n.i.	n.i.	n.i.	n.i.
	miR-199a-5p	–0.4026	n.i.	n.i.	n.i.
PRDX1	miR-199a-3p	–0.0142	n.i.	n.i.	n.i.
	miR-199a-5p	n.i.	n.i.	n.i.	–0.0196
DDAH1	miR-199a-3p	–0.0076	n.i.	n.i.	–0.0428
	miR-199a-5p	n.i.	n.i.	n.i.	n.i.
PRMT1	miR-199a-3p	n.i.	n.i.	n.i.	n.i.
	miR-199a-5p	n.i.	n.i.	n.i.	n.i.
VEGFA	miR-199a-3p	–0.20	n.i.	n.i.	–0.24
	miR-199a-5p	–0.1218	–0.71	n.i.	–0.1441

These scores are representative of an alignment of the seed sequence of the miRNA of interest with mRNA in humans; last column is miRSVR score in mouse. Akt indicates protein kinase B; CAV, caveolin; DDAH, dimethylarginine dimethylaminohydrolase; eNOS, endothelial NO synthase; HSP, ; miR/miRNA, microRNA; miRSVR, ; n.i., nonidentified matching sequences; NO, nitric oxide; PDK, pyruvate dehydrogenase kinase; PRDX, peroxiredoxin 1; PRMT, protein arginine N-methyltransferase; SOD, superoxide dismutase; and VEGFA, vascular endothelial growth factor A.

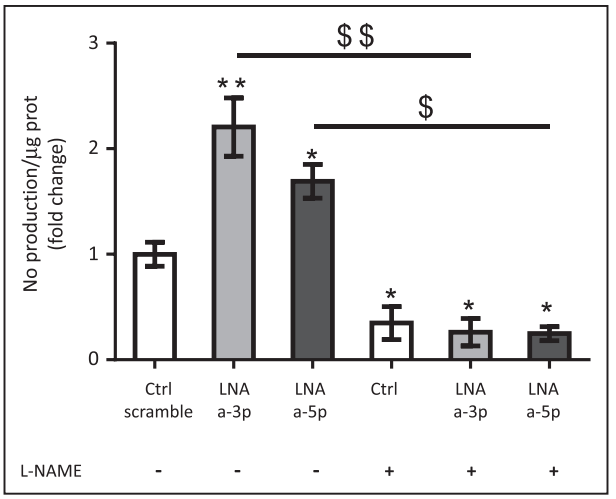

Figure 1. MicroRNA (miR) 199a-3p or -5p inhibition induces changes in nitric oxide (NO) production in endothelial cells. Bovine aortic endothelial cells were transfected with locked-nucleic acid (LNA) directed against miR-199a-3p or -199a-5p, and NO production was measured by electron paramagnetic resonance spin trapping after exposure to the spin trap colloid complex [(diethyldithiocarbamate)$_2$Fe(II)] for 45 min. Results are expressed as mean±SEM. Numbers of individual experiments are the following: Scramble, N=6; LNA a-3p, N=6; LNA a-5p, N=4; Scramble+ L-nitroarginine methyl ester (L-NAME), N=3; LNA a-3p+L-NAME, N=3 and LNA a-5p+L-NAME, N=3. *P<0.05 and **P<0.01 vs control (ctrl); $$P$<0.05 and $$$P$<0.01 vs L-NAME treatment.

-5p repression independently induced a prolonged increase in eNOS phosphorylation on Ser1177 (Figure 2A) after transfection of BAECs with either LNAs. These results correlated with a significant increase in Thr308 Akt phosphorylation 48 and 72 hours after the initiation of miRNA repression (Figure 2B). Similar results were observed in human aortic endothelial cells (data not shown). To prove a role of Akt in the LNA-supported increase in Ser1177 eNOS phosphorylation, we repeated the above experiments after silencing of Akt1,[33,34] the sole Akt isoform associated with eNOS[34] phosphorylation, and after treatment with the PI3K inhibitor LY294002. Akt1 siRNA treatment blunted the LNA-induced eNOS activation (Figure 2C), whereas LY294002 prevented both the phosphorylation of Akt on Thr308 and the increase in Ser1177 eNOS phosphorylation resulting from miR-199a-3p or -5p blockade (Figure 2D). Of note, we did not identify any effects of either LNA on the expression of PDK1 (Figure V in the online-only Data Supplement), the master kinase responsible for the activation of Akt (downstream of PI3K) identified as a potential miR-199a target (Table). In agreement with these results, transfection of miR-199a-3p or miR-199a-5p mimics evoked a decrease of eNOS activation through its phosphorylation on Ser1177 (Figure VIA in the online-only Data Supplement).

eNOS Phosphorylation on Thr495 is Modulated by miR-199a-3p and miR-199a-5p Repression Through the Calcineurin Pathway

Another well-known regulatory phosphorylation site within the eNOS sequence is the inactivating site, Thr495. We observed that LNA-based repression of miR-199a-3p and miR-199a-5p independently induced a decrease in the extent of Thr495 eNOS phosphorylation (Figure 3A). Importantly, we found that expression of calcineurin, the well-described phosphatase for Thr495 p-eNOS, was increased by >50% when miR-199a-3p or -5p were repressed (Figure 3B) in agreement with the identification of the calcineurin mRNA as a potential molecular target of miR-199a (Table). Accordingly, miR-199a-3p or -5p mimics transfection significantly reduced the phosphatase expression (Figure VIB in the online-only Data Supplement).

Repression of miR-199a-3p and miR-199a-5p Modulates the NO Bioavailability by Modulating SOD1 Expression

The above experiments indicated that miR-199a repression was associated with an increase in eNOS activity. We next evaluated whether the increase in NO abundance (Figure 1) could also arise from a decreased NO degradation because of a lesser reaction with superoxide anions ($O_2^{-}\cdot$). We first documented that repression of both miR-199a-3p and miR-199a-5p induced a marked reduction of $O_2^{-}\cdot$ levels in endothelial cells, as measured by dihydroethidium staining (Figure 4A). We also examined the expression of 2 ROS-regulating enzymes that we identified among the theoretical targets of miR-199a (Table), namely SOD1 and PRDX1, which catalyze the dismutation of $O_2^{-}\cdot$ into hydrogen peroxide (H_2O_2) and transforms H_2O_2 in oxygen and water, respectively. We found that both miR-199a-targeting LNAs led to a net increase in SOD1 (Figure 4B), whereas PRDX1 expression was only increased on transfection with miR-199a-5p-targeting LNA (Figure VII in the online-only Data Supplement).

Inhibition of miR-199a-5p Induces an Increase in VEGFA Protein Expression and Tube Formation

We next aimed to evaluate the effects of dedicated LNA on endothelial tube formation, a process known to be NO-mediated. This experiment was further guided by previous reports and our luciferase-based reporter assay identifying VEGFA (comprising all splicing variants) as a putative direct target of miR-199a-5p[35] (Table). Note that the absence of pairing between bovine VEGFA and miR-199a-3p is likely to account for the lack of regulation by LNA3p in BAECs. We confirmed an increase in VEGFA expression in cells transfected with miR-199a-5p inhibitor (but not miR-199a-3p; Figure 5A). Bevacizumab treatment of endothelial cells partially inhibited eNOS phosphorylation on Ser1177 observed following LNA5p transfection (Figure VIII in the online-only Data Supplement). In addition, the extent of precapillary tube formation, as assessed by plating endothelial cells on Matrigel and quantified with Image J software, was increased in response to miR-199a-targeting LNA, in particular when miR-199a-5p was repressed (Figure 5B and 5C).

Mice Treated With AntagomiRs Directed Against miR-199a-3p and miR-199a-5p Present an Improvement of Their Endothelial Function

To prove that miR-199a repression influences the amounts of bioactive NO in vivo, C57Bl6 male mice were treated with antagomiRs directed against miR-199a-3p or miR-199a-5p. At the time of euthanization (30 days after the

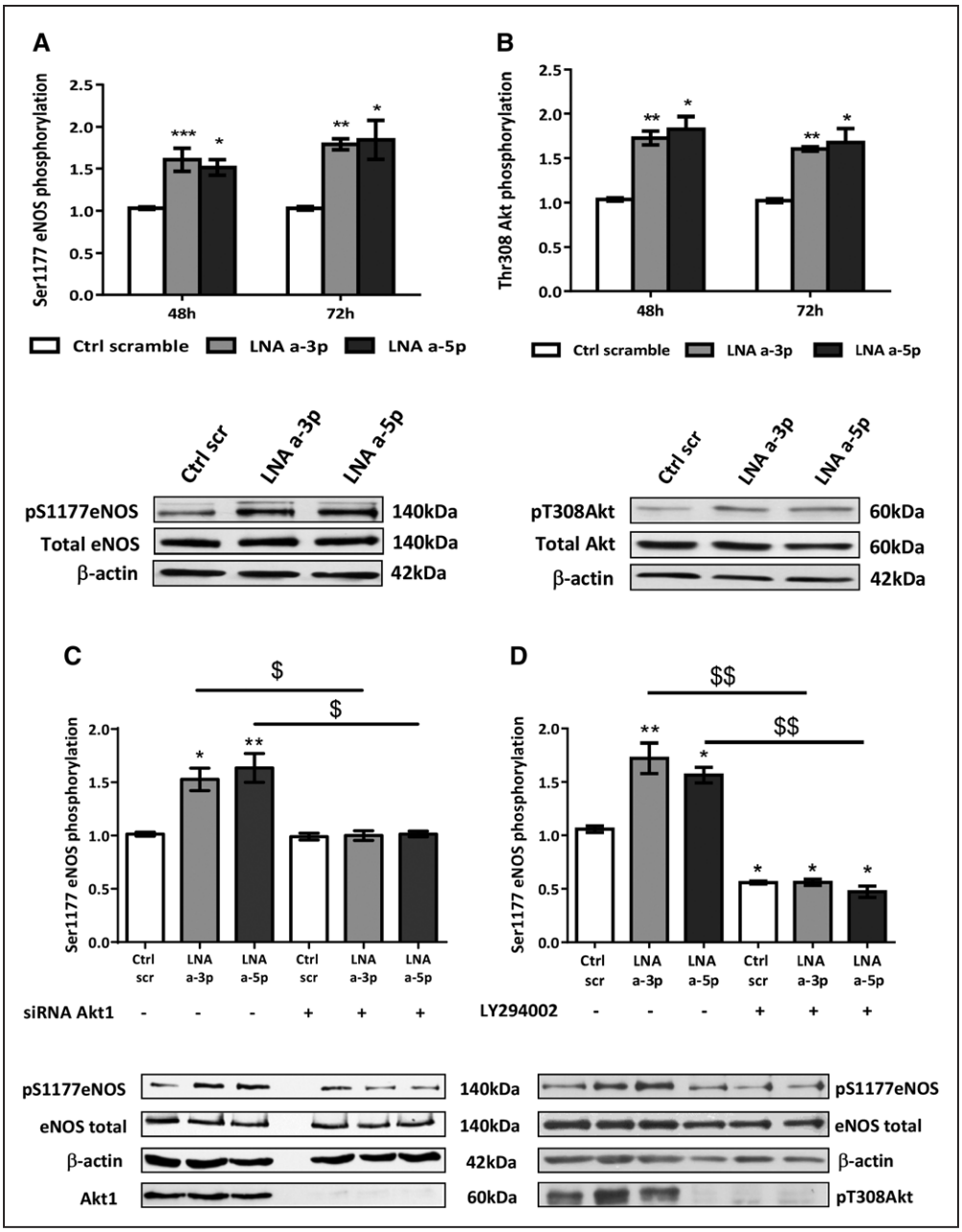

Figure 2. MicroRNA (miR) 199a-3p or -5p inhibition induces changes in Ser1177 eNOS (endothelial nitric oxide synthase) phosphorylation through modulation of the PI3K (phosphoinositide 3-kinase)/Akt (protein kinase B) pathway in endothelial cells. Bovine aortic endothelial cells (BAECs) were transfected with locked-nucleic acid (LNA) directed against miR-199a-3p or -199a-5p. Expression of pS1177eNOS and pT308Akt was detected by Western blotting and quantified (**A** and **B**, respectively). In some experiments, LNA-treated BAECs were also treated with Akt1 siRNA (**C**) or LY294002 (**D**), and expression of pS1177eNOS was detected by Western blotting and quantified. Results are expressed as mean±SEM. Numbers of individual experiments are the following: N=10 for each condition for graphs **A** and **B** and N=4 (without Akt inhibitor) or 3 (with Akt inhibitor) for graphs **C** and **D**. **P*<0.05, ***P*<0.01 and ****P*<0.001 vs scramble control (ctrl scr); $*P*<0.05 and $$*P*<0.01 vs Akt inhibition treatment.

initiation of in vivo antagomiR administration), plasma was collected to verify the expression of circulating miRs. A specific decrease of the targeted miR was observed without significant alterations in the expression of the opposite strand (Figure IIC and IID in the online-only Data Supplement). Isolated aorta presented a significantly larger NO-dependent relaxation as measured in KCl precontracted vessels (versus vessels from mice treated with saline or scramble sequence; Figure 6A). These results were further validated by the detection of increased levels of circulating hemoglobin-NO (HbNO) in the venous blood of antagomiR-treated mice (Figure 6B). Also, EPR measurements of $O_2^{-}\cdot$ production in aortic rings obtained from mice treated with antagomiRs against miR-199a-3p or -5p revealed a net reduction in $O_2^{-}\cdot$ levels (versus control conditions; Figure 6C). In agreement with the data obtained in cultured endothelial cells, an increase of eNOS phosphorylation on Ser1177 (Figure 6D) was observed in the aorta of antagomiR-treated mice (versus control mice). Moreover, an increase of calcineurin and SOD1 expression (Figure 6E

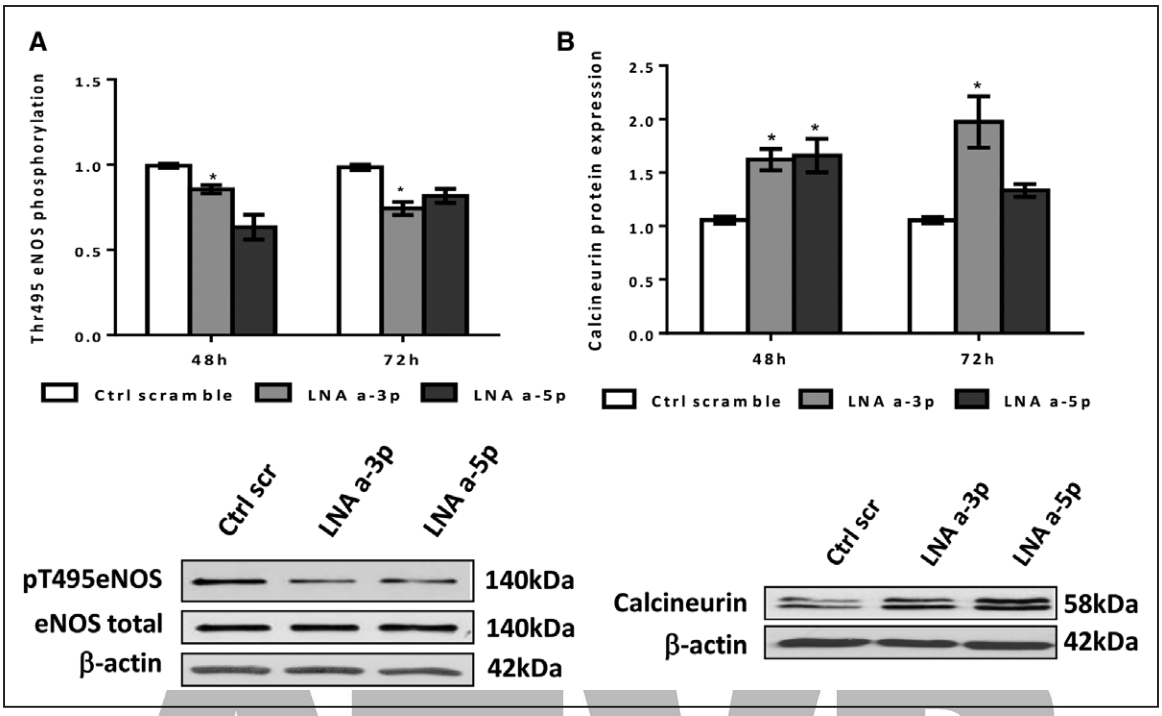

Figure 3. MicroRNA (miR) 199a-3p or -5p inhibition induces changes in Thr495 eNOS (endothelial nitric oxide synthase) phosphorylation through calcineurin phosphatase modulation in endothelial cells. Bovine aortic endothelial cells were transfected with locked-nucleic acid (LNA) directed against miR-199a-3p or -199a-5p. Expression of pT495eNOS and calcineurin was detected by Western blotting and quantified (**A** and **B**, respectively). Results are expressed as mean±SEM. Numbers of individual experiments are the following: Scramble, N=5; LNA a-3p, N= 4; LNA a-5p, N=4. (**lower**) representative phosphoblot of endothelial extracts at 48 h **P*<0.05 vs scramble control (ctrl scr).

and 6F) was also identified in isolated vessels further supporting our in vitro data. Finally, as observed in cultured endothelial cells, antagomiR-treated and control mice presented the same levels of ADMA in their plasma (Figure IVD in the online-only Data Supplement).

miR-199a-3p and miR-199a-5p are Increased in Mice Model of Hypertension

To verify the implication of miR-199a in pathological conditions, mice were implanted with angiotensin infusing minipump (2 mg/kg per day) for 14 days, a well-described model of hypertension and cardiac hypertrophy.[29] Heart and aorta isolated from these mice exhibited a larger expression of both mature miR-199a. Interestingly, a dysregulation of miR expression was only observed for miR-199a-5p in the plasma of hypertensive mice (Figure IX in the online-only Data Supplement).

Discussion

miRNAs derived from the precursor miR-199a are known to play critical roles in the maintenance of cardiac homeostasis.[19,36] Our study reveals that both mature miRNAs (namely miR-199a-3p and miR-199a-5p) also participate in a redundant network of eNOS regulation in the endothelium (see Graphic Abstract). In particular, we highlighted how inhibition of miR-199a-3p and miR-199a-5p independently increases NO bioavailability by promoting eNOS enzymatic activity and reducing NO degradation, thereby, supporting VEGFA-induced endothelial tubulogenesis and modulating vessel contractile tone.

miR-199a is well conserved in different species[37] and in the human genome, it is encoded by 2 loci within introns of the *DNM* (dynamin 2 and 3), miR-199a-1 in chromosome 19 and mir-199a-2 in chromosome 1. Classically, 1 of the 2 strands derived from the precursor is considered as mature (miR) and the other one (miR*) is degraded, the ratio miR/miR* varying according to the rate of degradation of the immature strand. There is, however, growing evidence that both strands might exhibit regulatory activities.[38] Accordingly, both strands (-5p and -3p) from pre-miR-199a can form mature miRNAs that may behave differently depending on the pathological contexts.[37] In this study, we found that both miRNAs, miR-199a-3p and miR-199a-5p were significantly expressed in endothelial cells and independently regulated NO production. Based on various in vitro and ex vivo assays, we found that NO availability was increased through an increased eNOS enzymatic activity, an effect further reinforced by reduced superoxide production.

Strikingly, we identified that the eNOS phosphorylation status was altered not only on the stimulatory Ser1177 site but also on the inactivating Thr495 site. We identified the stimulatory effects of miR-199a-3p and -5p-targeting LNAs on the PI3K/Akt pathway and on the calcineurin phosphatase as the respective triggers of this mode of eNOS activation. The upregulation of calcineurin on miR-199a blockade was in agreement with the in silico identification of calcineurin-encoding gene as a theoretical target of this miRNA (see Table) and further validated by a dedicated luciferase-based reporter assay. By contrast, although pharmacological inhibition of PI3K and Akt genetic silencing proved the

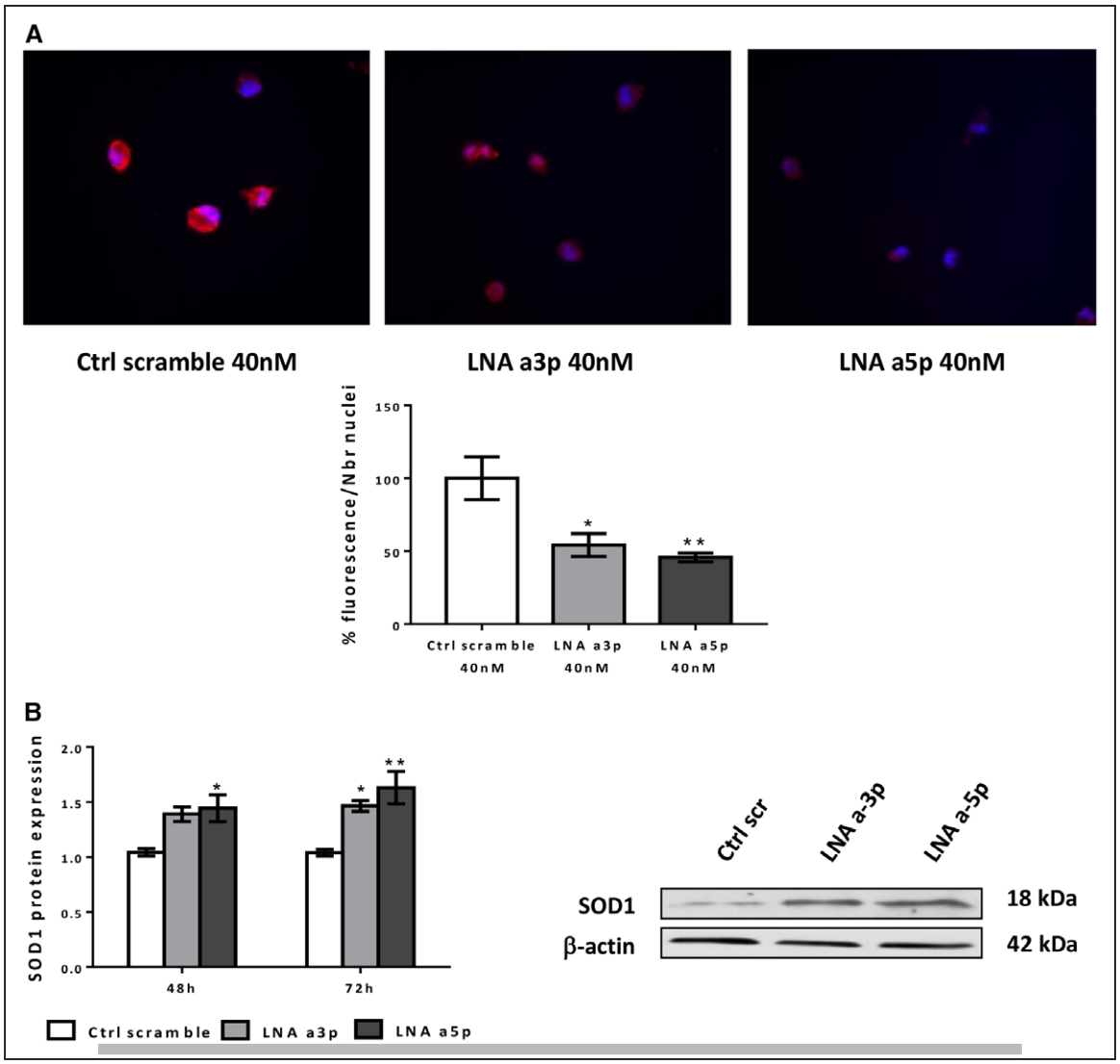

Figure 4. MicroRNA (miR) 199a-3p or -5p inhibition induces a reduction in superoxide anion production in endothelial cells through an increase in SOD1 (superoxide dismutase 1) expression. Bovine aortic endothelial cells were transfected with locked-nucleic acid (LNA) directed against miR-199a-3p or -199a-5p, and superoxide anion levels were assessed by dihydroethidium (DHE) staining (**A**, red) and quantified (see bar graph); nucleus was counterstained using Hoechst dye (**A**, blue). Expression of SOD1 was detected by Western blotting and quantified (**B**). Results are expressed as mean±SEM. Numbers of individual experiments are the following: N=3 for each condition for DHE staining and N=4 for each condition for SOD1 quantification. *P<0.05 and **P<0.01 vs control (ctrl). Scr indicates scramble.

role of this pathway on Ser1177 phosphorylation, we did not observe changes in the abundance of Akt (or PDK1) on LNA treatment (despite favorable matching scores between miRNAs sequences and Akt mRNA [Table]). Further studies are warranted to identify possible targets involved in the regulation of the PI3K/AKT pathway. Interestingly, the miR-199a-mediated regulation of Akt was recently highlighted in mouse heart as supportive of physiological cardiac hypertrophy,[21] myoblast differentiation[39] and cardiomyocyte proliferation,[40] and survival under ischemic stress.[41] Interestingly, besides increased eNOS activity resulting from increased Ser1177 phosphorylation and Thr495 dephosphorylation, our study also provides evidence that miR-199 blockade can increase NO bioavailability by preventing its inactivation. We actually found that SOD was increased on repression of miR-199a-3p or -5p, thereby, supporting a reduced oxidative stress and thus promoting an increase in NO availability. It is also worth noting that although similar effects (ie, changes in eNOS phosphorylation and SOD activity) were obtained with LNA targeting either miR-199a form, repression of miR-199a-5p exhibited a significantly stronger effect on the upregulation of PRDX1 (another ROS detoxifying enzyme) than on miR-199-3p blockade. A large effect of miR-199a-5p-targeting LNA was observed on VEGFA expression and endothelial tube formation. However, we cannot exclude that in human endothelial cells, miR-199a-3p could also regulate VEGFA to some extent. The respective contribution of VEGFA overexpression to eNOS activation in our experimental setup is actually difficult to delineate because Akt phosphorylation itself (a main driver of eNOS phosphorylation) is independently increased in response to LNA treatment. Nevertheless, altogether, these data reinforce

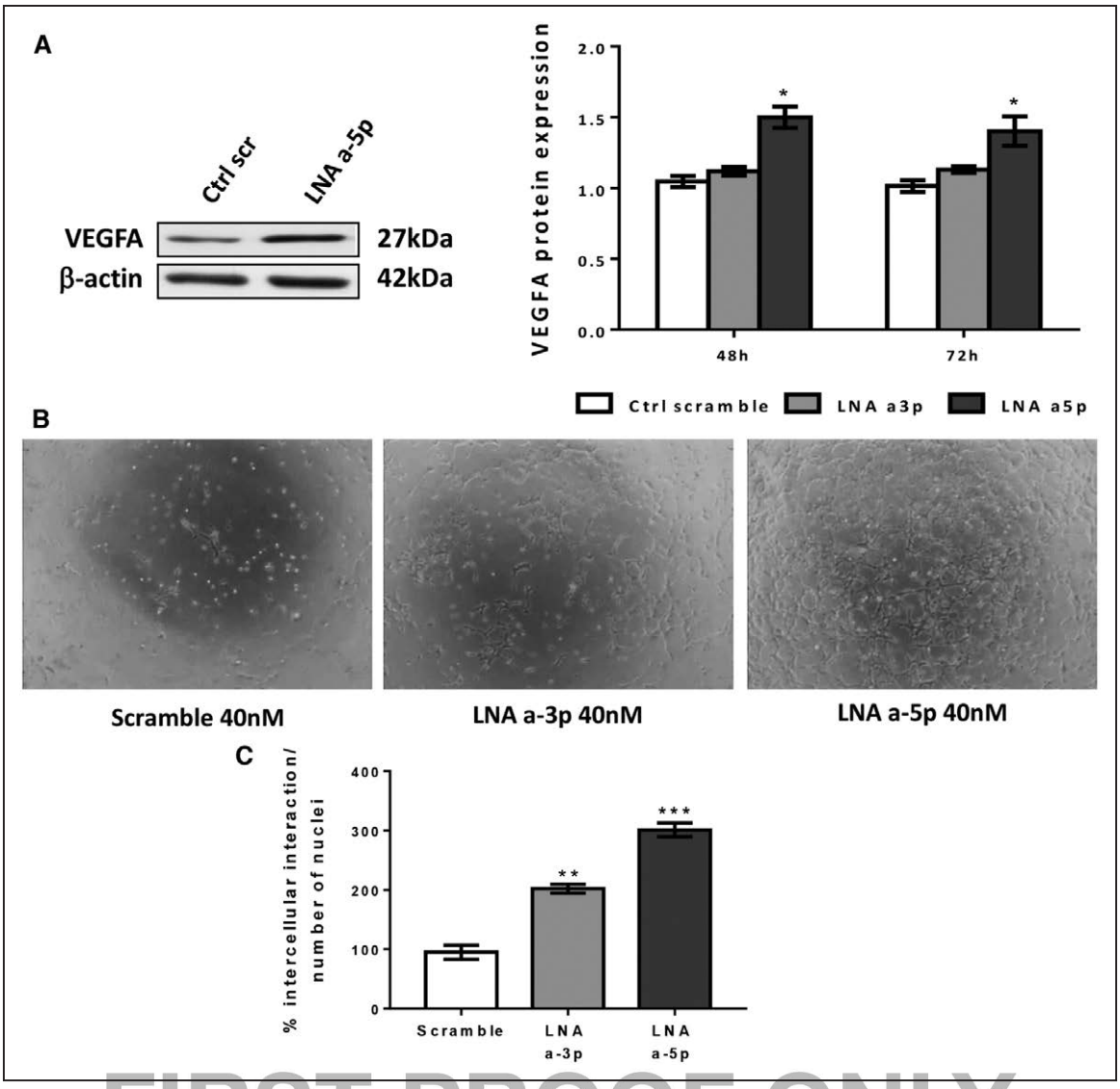

Figure 5. MicroRNA (miR) 199a-3p or -5p inhibition induces an increase of VEGFA (vascular endothelial growth factor A) expression and endothelial tube formation. Bovine aortic endothelial cells (BAECs) were transfected with locked-nucleic acid (LNA) directed against miR-199a-3p or -199a-5p, and expression of VEGFA was detected by Western blotting and quantified (**A**). In some experiments, LNA-treated BAECs were collected and mixed with equal volume of Matrigel to assess tube formation (**B**). Results are expressed as mean±SEM. Numbers of dual experiments are the following: N=4 for each condition for VEGF quantification and Matrigel assay. **P*<0.05, ***P*<0.01, and ****P*<0.001 vs scramble control (ctrl scr).

the redundant aspect of miR-199a regulation on the endothelial NOS/NO pathway.

Importantly, in our study, the effects of chronic mouse exposure to anti-miR-199a antagomiRs further provided several sets of evidence supporting a relevant role of miR-199a in in vivo settings. We have indeed observed a dramatic increase in the relaxation of vessels isolated from antagomiR-treated mice together with a reduced superoxide production and an increased circulating HbNO reflecting a global increase in NO availability. Modifications of eNOS phosphorylation, calcineurin, and SOD expression also argue in favor of a role of miR-199a-3p and 5p in vivo. It should be noted that previous publications have reported effects of either miR-199a-5p or -3p on eNOS activity through changes in Cav expression.[42] In our hands, such regulation could not be observed, possibly suggesting differential miRNA regulation processes in different cell types or physio-pathological contexts. Also, we failed to document a link between the expression of miR-199a and the abundance of the endogenous eNOS inhibitor ADMA (and of the related producing/metabolizing enzymes), as previously reported in cardiomyocytes.[23] However, the latter observation could result from differential targeting according to the cellular context (ie, cardiac myocytes versus endothelial cells) or nonspecific effects resulting from the overexpression of pre-miR-199a.

Taken together, our results indicate that miRNAs matured from miR-199a, working potentially in cluster, take part in a redundant network of regulation of the NOS/NO pathway in the endothelium and modulate key endothelial functions, including angiogenesis and vascular tone. miR-199a has, therefore, to be added to the short list of miRNAs reported to modulate eNOS expression or activity, such as miR-155 and miR-21.[43] Our observations are in agreement with studies documenting that miRNAs often fine-tune cellular homeostasis

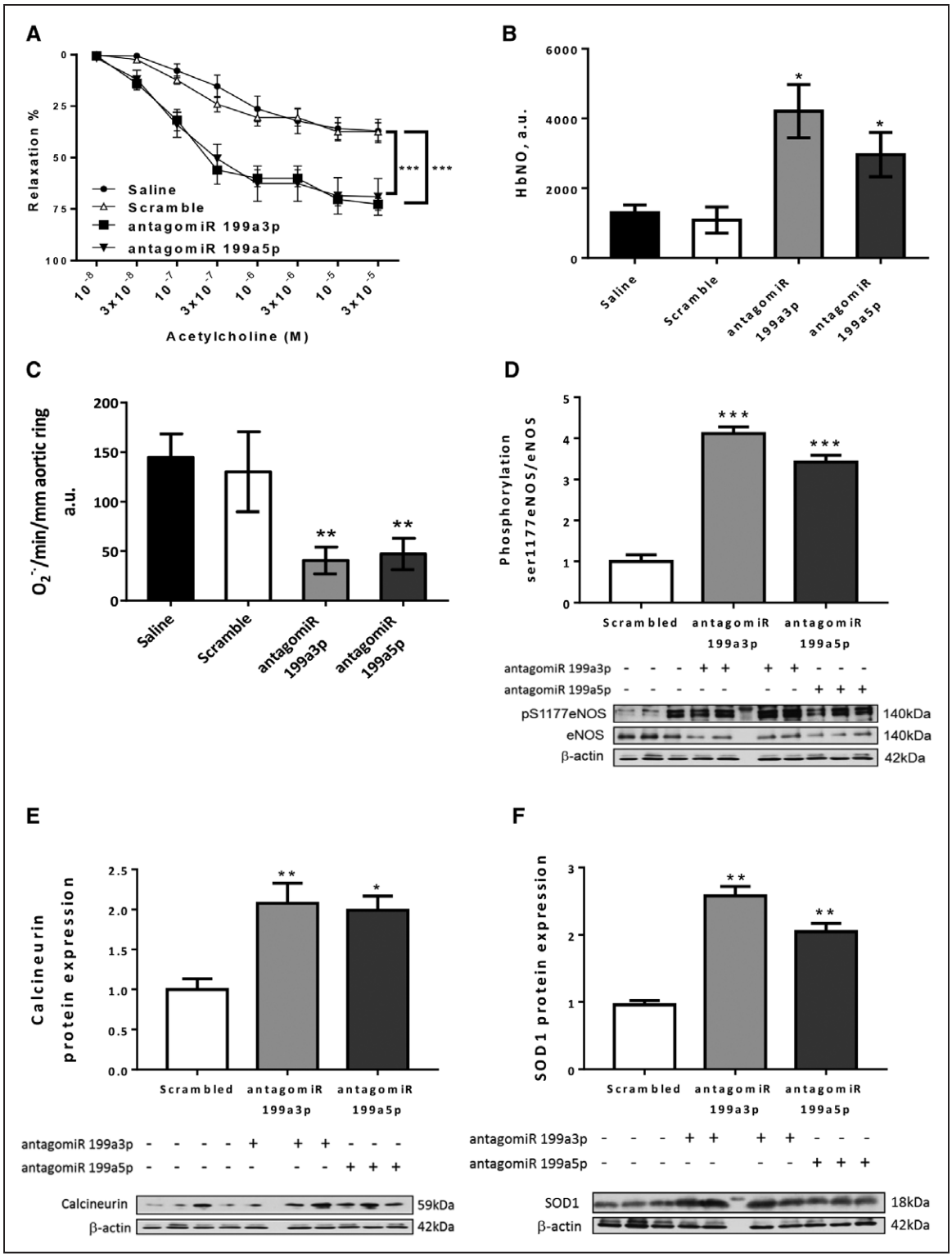

Figure 6. Vessels isolated from mice treated with microRNA (miR)-199a-3p or -199a-5p inhibitors exhibit an increased endothelium-dependent nitric oxide (NO)-dependent relaxation. Mice were treated on 3 consecutive days with antagomiRs (75 mg/kg per day) against miR 199a-3p/-5p and euthanized 30 d after treatment. Dose-dependent effects of acetylcholine on mouse aorta relaxation determined on a wire myograph (**A**). Venous blood from these mice (**B**) and aortic rings (**C**) were also collected to assess hemoglobin-NO (HbNO) and superoxide anion levels, respectively, by electron paramagnetic resonance. Expression of pS1177eNOS (endothelial NO synthase), calcineurin, and SOD1 (superoxide dismutase 1) was detected by Western blotting and quantified (**D**–**F**). Results are expressed as mean±SEM of at least 5 animals for physiological experiments and 6 (**D**–**E**) or 4 (**F**) animals for Western blot experiments **P*<0.05, ***P*<0.01 and ****P*<0.001 vs indicated controls (saline or scramble).

through intercrossed regulatory networks controlled by multiple miRNAs.[44] More specifically, the dysregulation of both mature arms of miR-199a initially reported in heart may now be extended to the vascular tissues, thereby opening new perspectives of treatment. Our study actually provides evidence that new therapeutic opportunities may stem from altering these subtle modes of regulation in blood vessels, for instance through the use of endothelial-directed aptamer inhibitors or miRNA-sponges.

Acknowledgments

C. Dessy is a senior research associate of the FRS-FNRS. We thank Delphine De Mulder for her technical help.

Sources of Funding

The support of Humanitas Research Hospital and the National Research Council of Italy is acknowledged

Disclosures

None.

References

1. Lundberg JO, Gladwin MT, Weitzberg E. Strategies to increase nitric oxide signalling in cardiovascular disease. *Nat Rev Drug Discov*. 2015;14:623–641. doi: 10.1038/nrd4623
2. Balligand JL, Feron O, Dessy C. eNOS activation by physical forces: from short-term regulation of contraction to chronic remodeling of cardiovascular tissues. *Physiol Rev*. 2009;89:481–534. doi: 10.1152/physrev.00042.2007
3. Roviezzo F, Cuzzocrea S, Di Lorenzo A, Brancaleone V, Mazzon E, Di Paola R, Bucci M, Cirino G. Protective role of PI3-kinase-Akt-eNOS signalling pathway in intestinal injury associated with splanchnic artery occlusion shock. *Br J Pharmacol*. 2007;151:377–383. doi: 10.1038/sj.bjp.0707233
4. Brouet A, Sonveaux P, Dessy C, Moniotte S, Balligand JL, Feron O. Hsp90 and caveolin are key targets for the proangiogenic nitric oxide-mediated effects of statins. *Circ Res*. 2001;89:866–873.
5. Brouet A, Sonveaux P, Dessy C, Balligand JL, Feron O. Hsp90 ensures the transition from the early Ca2+-dependent to the late phosphorylation-dependent activation of the endothelial nitric-oxide synthase in vascular endothelial growth factor-exposed endothelial cells. *J Biol Chem*. 2001;276:32663–32669. doi: 10.1074/jbc.M101371200
6. Qian J, Fulton D. Post-translational regulation of endothelial nitric oxide synthase in vascular endothelium. *Front Physiol*. 2013;4:347. doi: 10.3389/fphys.2013.00347
7. Leiper J, Nandi M. The therapeutic potential of targeting endogenous inhibitors of nitric oxide synthesis. *Nat Rev Drug Discov*. 2011;10:277–291. doi: 10.1038/nrd3358
8. Pacher P, Szabó C. Role of peroxynitrite in the pathogenesis of cardiovascular complications of diabetes. *Curr Opin Pharmacol*. 2006;6:136–141. doi: 10.1016/j.coph.2006.01.001
9. Pacher P, Szabo C. Role of the peroxynitrite-poly(ADP-ribose) polymerase pathway in human disease. *Am J Pathol*. 2008;173:2–13. doi: 10.2353/ajpath.2008.080019
10. Williams IL, Wheatcroft SB, Shah AM, Kearney MT. Obesity, atherosclerosis and the vascular endothelium: mechanisms of reduced nitric oxide bioavailability in obese humans. *Int J Obes Relat Metab Disord*. 2002;26:754–764. doi: 10.1038/sj.ijo.0801995
11. Agnoletti L, Curello S, Bachetti T, Malacarne F, Gaia G, Comini L, Volterrani M, Bonetti P, Parrinello G, Cadei M, Grigolato PG, Ferrari R. Serum from patients with severe heart failure downregulates eNOS and is proapoptotic: role of tumor necrosis factor-alpha. *Circulation*. 1999;100:1983–1991.
12. Oemar BS, Tschudi MR, Godoy N, Brovkovich V, Malinski T, Lüscher TF. Reduced endothelial nitric oxide synthase expression and production in human atherosclerosis. *Circulation*. 1998;97:2494–2498.
13. Li H, Wallerath T, Münzel T, Förstermann U. Regulation of endothelial-type NO synthase expression in pathophysiology and in response to drugs. *Nitric Oxide*. 2002;7:149–164.
14. Sena CM, Pereira AM, Seiça R. Endothelial dysfunction - a major mediator of diabetic vascular disease. *Biochim Biophys Acta*. 2013;1832:2216–2231. doi: 10.1016/j.bbadis.2013.08.006
15. Duan Z, Choy E, Harmon D, Liu X, Susa M, Mankin H, Hornicek F. MicroRNA-199a-3p is downregulated in human osteosarcoma and regulates cell proliferation and migration. *Mol Cancer Ther*. 2011;10:1337–1345. doi: 10.1158/1535-7163.MCT-11-0096
16. He J, Jing Y, Li W, Qian X, Xu Q, Li FS, Liu LZ, Jiang BH, Jiang Y. Roles and mechanism of miR-199a and miR-125b in tumor angiogenesis. *PLoS One*. 2013;8:e56647. doi: 10.1371/journal.pone.0056647
17. van Rooij E, Sutherland LB, Liu N, Williams AH, McAnally J, Gerard RD, Richardson JA, Olson EN. A signature pattern of stress-responsive microRNAs that can evoke cardiac hypertrophy and heart failure. *Proc Natl Acad Sci USA*. 2006;103:18255–18260. doi: 10.1073/pnas.0608791103
18. van Rooij E, Marshall WS, Olson EN. Toward microRNA-based therapeutics for heart disease: the sense in antisense. *Circ Res*. 2008;103:919–928. doi: 10.1161/CIRCRESAHA.108.183426
19. Catalucci D, Latronico MV, Condorelli G. MicroRNAs control gene expression: importance for cardiac development and pathophysiology. *Ann N Y Acad Sci*. 2008;1123:20–29. doi: 10.1196/annals.1420.004
20. Li Z, Song Y, Liu L, Hou N, An X, Zhan D, Li Y, Zhou L, Li P, Yu L, Xia J, Zhang Y, Wang J, Yang X. miR-199a impairs autophagy and induces cardiac hypertrophy through mTOR activation. *Cell Death Differ*. 2017;24:1205–1213. doi: 10.1038/cdd.2015.95
21. Li Z, Liu L, Hou N, Song Y, An X, Zhang Y, Yang X, Wang J. miR-199-sponge transgenic mice develop physiological cardiac hypertrophy. *Cardiovasc Res*. 2016;110:258–267. doi: 10.1093/cvr/cvw052
22. Song XW, Li Q, Lin L, Wang XC, Li DF, Wang GK, Ren AJ, Wang YR, Qin YW, Yuan WJ, Jing Q. MicroRNAs are dynamically regulated in hypertrophic hearts, and miR-199a is essential for the maintenance of cell size in cardiomyocytes. *J Cell Physiol*. 2010;225:437–443. doi: 10.1002/jcp.22217
23. Haghikia A, Missol-Kolka E, Tsikas D, Venturini L, Brundiers S, Castoldi M, Muckenthaler MU, Eder M, Stapel B, Thum T, Haghikia A, Petrasch-Parwez E, Drexler H, Hilfiker-Kleiner D, Scherr M. Signal transducer and activator of transcription 3-mediated regulation of miR-199a-5p links cardiomyocyte and endothelial cell function in the heart: a key role for ubiquitin-conjugating enzymes. *Eur Heart J*. 2011;32:1287–1297. doi: 10.1093/eurheartj/ehq369
24. Craps J, Wilvers C, Joris V, De Jongh B, Vanderstraeten J, Lobysheva I, Balligand JL, Sonveaux P, Gilon P, Many MC, Gérard AC, Colin IM. Involvement of nitric oxide in iodine deficiency-induced microvascular remodeling in the thyroid gland: role of nitric oxide synthase 3 and ryanodine receptors. *Endocrinology*. 2015;156:707–720. doi: 10.1210/en.2014-1729
25. van Rooij E, Sutherland LB, Thatcher JE, DiMaio JM, Naseem RH, Marshall WS, Hill JA, Olson EN. Dysregulation of microRNAs after myocardial infarction reveals a role of miR-29 in cardiac fibrosis. *Proc Natl Acad Sci USA*. 2008;105:13027–13032. doi: 10.1073/pnas.0805038105
26. Thum T, Gross C, Fiedler J, et al. MicroRNA-21 contributes to myocardial disease by stimulating MAP kinase signalling in fibroblasts. *Nature*. 2008;456:980–984. doi: 10.1038/nature07511
27. Caballero-Garrido E, Pena-Philippides JC, Lordkipanidze T, Bragin D, Yang Y, Erhardt EB, Roitbak T. *In Vivo* inhibition of miR-155 promotes recovery after experimental mouse stroke. *J Neurosci*. 2015;35:12446–12464. doi: 10.1523/JNEUROSCI.1641-15.2015
28. Gélinas R, Mailleux F, Dontaine J, et al. AMPK activation counteracts cardiac hypertrophy by reducing O-GlcNAcylation. *Nat Commun*. 2018;9:374. doi: 10.1038/s41467-017-02795-4
29. Desjardins F, Lobysheva I, Pelat M, Gallez B, Feron O, Dessy C, Balligand JL. Control of blood pressure variability in caveolin-1-deficient mice: role of nitric oxide identified *in vivo* through spectral analysis. *Cardiovasc Res*. 2008;79:527–536. doi: 10.1093/cvr/cvn080
30. Rouaud F, Romero-Perez M, Wang H, Lobysheva I, Ramassamy B, Henry E, Tauc P, Giacchero D, Boucher JL, Deprez E, Rocchi S, Slama-Schwok A. Regulation of NADPH-dependent nitric oxide and reactive oxygen species signalling in endothelial and melanoma cells by a photoactive NADPH analogue. *Oncotarget*. 2014;5:10650–10664. doi: 10.18632/oncotarget.2525
31. Ghisdal P, Gomez JP, Morel N. Action of a NO donor on the excitation-contraction pathway activated by noradrenaline in rat superior mesenteric artery. *J Physiol*. 2000;522(pt 1):83–96.
32. Saliez J, Bouzin C, Rath G, Ghisdal P, Desjardins F, Rezzani R, Rodella LF, Vriens J, Nilius B, Feron O, Balligand JL, Dessy C. Role of caveolar compartmentation in endothelium-derived hyperpolarizing

factor-mediated relaxation: Ca2+ signals and gap junction function are regulated by caveolin in endothelial cells. *Circulation*. 2008;117:1065–1074. doi: 10.1161/CIRCULATIONAHA.107.731679
33. Somanath PR, Razorenova OV, Chen J, Byzova TV. Akt1 in endothelial cell and angiogenesis. *Cell Cycle*. 2006;5:512–518. doi: 10.4161/cc.5.5.2538.
34. Yu H, Littlewood T, Bennett M. Akt isoforms in vascular disease. *Vascul Pharmacol*. 2015;71:57–64. doi: 10.1016/j.vph.2015.03.003
35. Hsu CY, Hsieh TH, Tsai CF, Tsai HP, Chen HS, Chang Y, Chuang HY, Lee JN, Hsu YL, Tsai EM. miRNA-199a-5p regulates VEGFA in endometrial mesenchymal stem cells and contributes to the pathogenesis of endometriosis. *J Pathol*. 2014;232:330–343. doi: 10.1002/path.4295
36. Neppl RL, Wang DZ. The myriad essential roles of microRNAs in cardiovascular homeostasis and disease. *Genes Dis*. 2014;1:18–39. doi: 10.1016/j.gendis.2014.06.003
37. Gu S, Chan WY. Flexible and versatile as a chameleon-sophisticated functions of microRNA-199a. *Int J Mol Sci*. 2012;13:8449–8466. doi: 10.3390/ijms13078449
38. Guo L, Lu Z. The fate of miRNA* strand through evolutionary analysis: implication for degradation as merely carrier strand or potential regulatory molecule? *PLoS One*. 2010;5:e11387. doi: 10.1371/journal.pone.0011387
39. Jia L, Li YF, Wu GF, Song ZY, Lu HZ, Song CC, Zhang QL, Zhu JY, Yang GS, Shi XE. MiRNA-199a-3p regulates C2C12 myoblast differentiation through IGF-1/AKT/mTOR signal pathway. *Int J Mol Sci*. 2013;15:296–308. doi: 10.3390/ijms15010296
40. Condorelli G, Latronico MV, Cavarretta E. MicroRNAs in cardiovascular diseases: current knowledge and the road ahead. *J Am Coll Cardiol*. 2014;63:2177–2187. doi: 10.1016/j.jacc.2014.01.050
41. Park KM, Teoh JP, Wang Y, Broskova Z, Bayoumi AS, Tang Y, Su H, Weintraub NL, Kim IM. Carvedilol-responsive microRNAs, miR-199a-3p and -214 protect cardiomyocytes from simulated ischemia-reperfusion injury. *Am J Physiol Heart Circ Physiol*. 2016;311:H371–H383. doi: 10.1152/ajpheart.00807.2015
42. Zeng J, Chen L, Chen B, Lu K, Belguise K, Wang X, Yi B. MicroRNA-199a-5p regulates the proliferation of pulmonary microvascular endothelial cells in hepatopulmonary syndrome. *Cell Physiol Biochem*. 2015;37:1289–1300. doi: 10.1159/000430252
43. Nishiguchi T, Imanishi T, Akasaka T. MicroRNAs and cardiovascular diseases. *Biomed Res Int*. 2015;2015:682857. doi: 10.1155/2015/682857
44. Bracken CP, Scott HS, Goodall GJ. A network-biology perspective of microRNA function and dysfunction in cancer. *Nat Rev Genet*. 2016;17:719–732. doi: 10.1038/nrg.2016.134

Highlights

- MicroRNA (miR)-199a-3p and miR-199a-5p independently regulate the NOS (nitric oxide synthase)/NO pathway through modulation of NOS activity.
- miR-199a-3p and -5p modulate oxidative stress reinforcing their independent impact on NO bioavailability.
- Our data demonstrate that miR-199a-3p and miR-199a-5p take part in a redundant network of regulation in the endothelium paving the way for new therapeutic opportunities.

Arteriosclerosis, Thrombosis, and Vascular Biology

JOURNAL OF THE AMERICAN HEART ASSOCIATION

MicroRNA-199a-3p and MicroRNA-199a-5p Take Part to a Redundant Network of Regulation of the NOS (NO Synthase)/NO Pathway in the Endothelium

Virginie Joris, Elvira Leon Gomez, Lisa Menchi, Irina Lobysheva, Vittoria Di Mauro, Hrag Esfahani, Gianluigi Condorelli, Jean-Luc Balligand, Daniele Catalucci and Chantal Dessy

Arterioscler Thromb Vasc Biol. published online July 5, 2018;
Arteriosclerosis, Thrombosis, and Vascular Biology is published by the American Heart Association, 7272 Greenville Avenue, Dallas, TX 75231

Print ISSN: 1079-5642. Online ISSN: 1524-4636

The online version of this article, along with updated information and services, is located on the World Wide Web at:
http://atvb.ahajournals.org/content/early/2018/07/03/ATVBAHA.118.311145

Data Supplement (unedited) at:
http://atvb.ahajournals.org/content/suppl/2018/07/03/ATVBAHA.118.311145.DC1

Suppl fig I

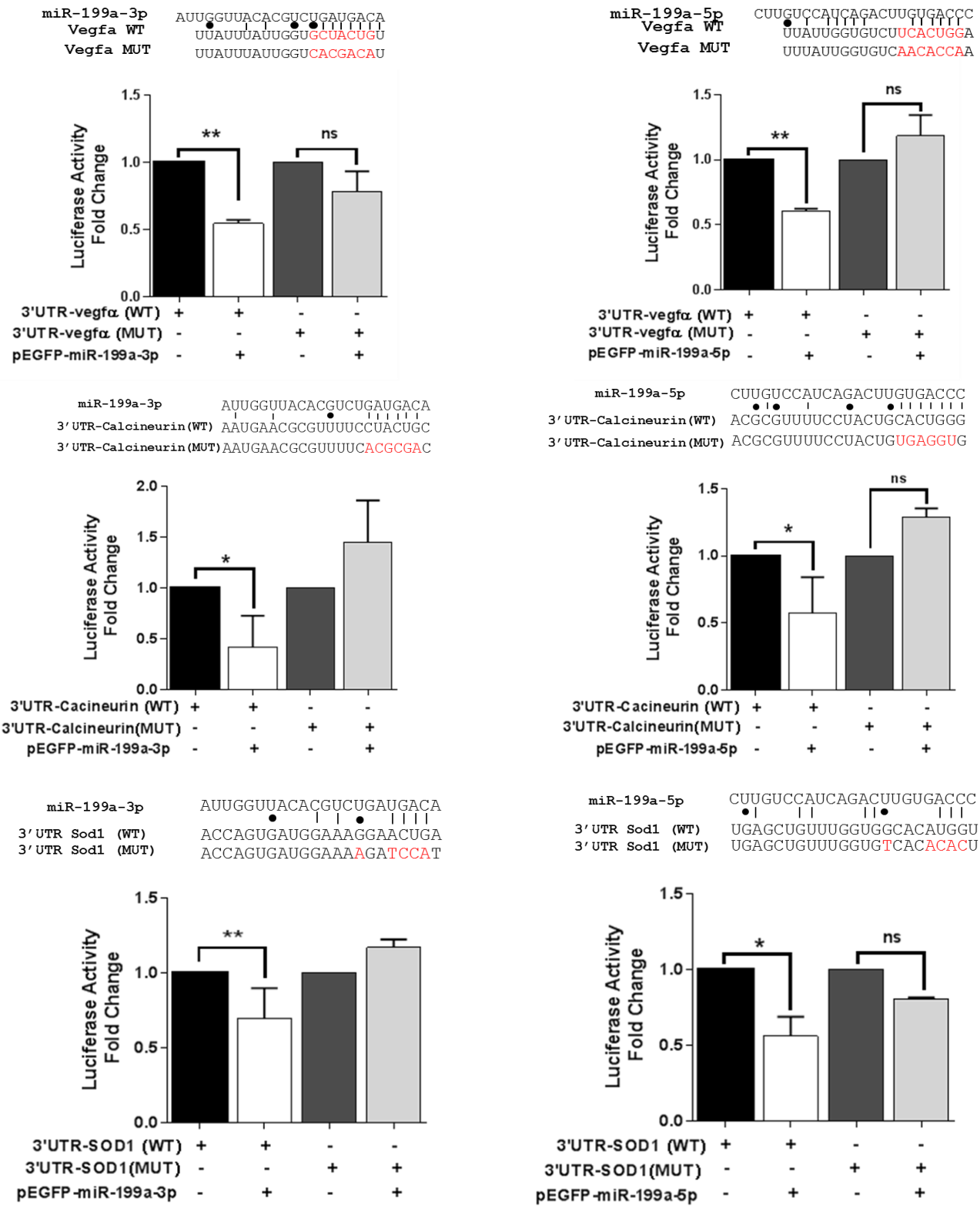

Figure I: Luciferase-based reporter assays highlight matching sequence between miR-199a-3p or miR-199a-5p and predicted mRNAs targets including VEGFA, Calcineurin and SOD1. HeK-293T cells were transfected with pmiRGlo-3'UTR and pcDNA6.2-GW/EmGFP-miR-199a/a* plasmids. 48h post transfection, cells were lysed and luciferase activity was measured using the Nano-Glo® Dual-Luciferase® Reporter (NanoDLR™) Assay System. Results are expressed as mean ± SEM of 3 individual experiments. *, *P.*<0.05 and **, *P.*<0.01 *vs.* control (WT alone)

Suppl fig II

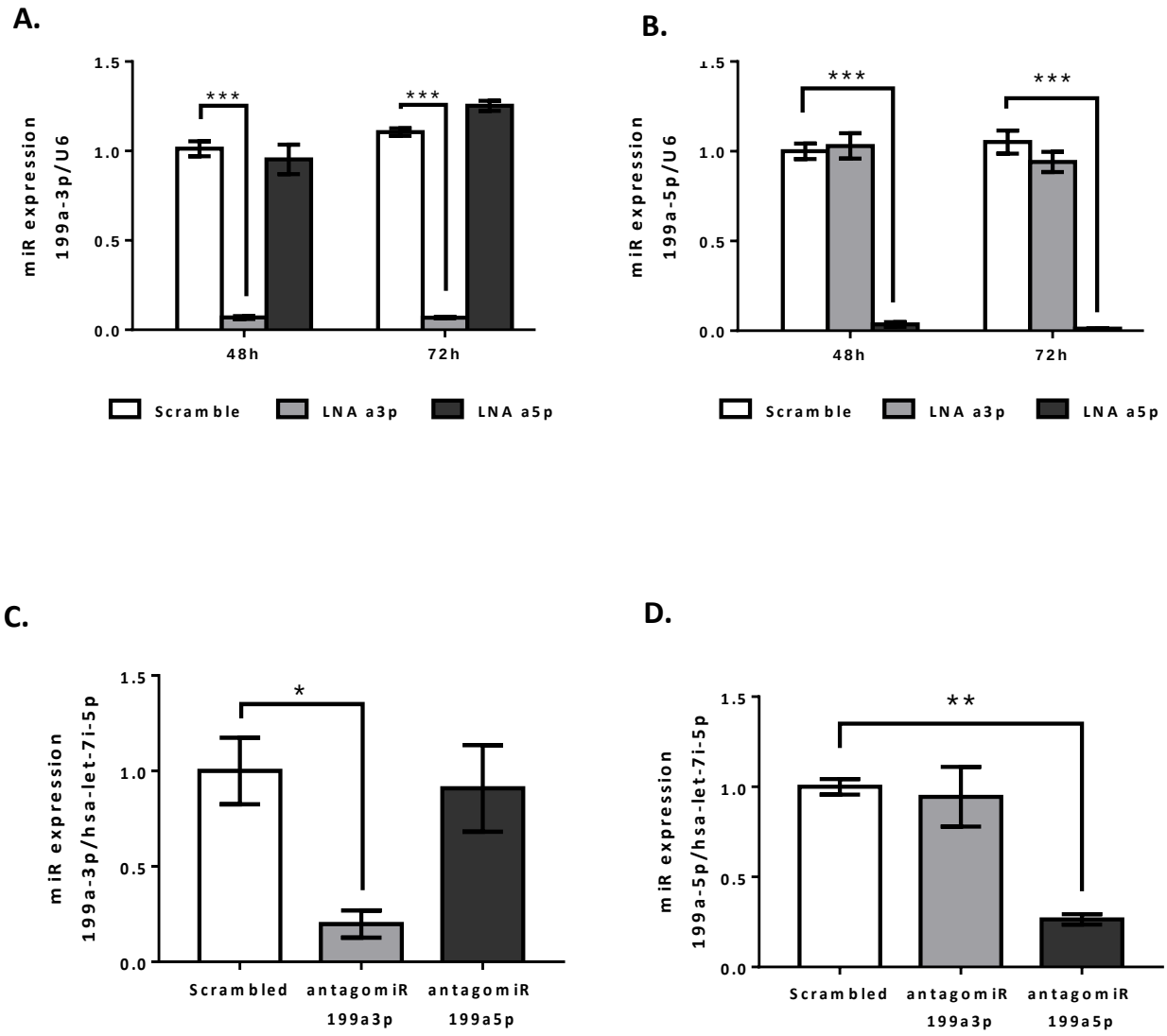

Figure II: Locked-Nucleic Acid and antagomiRs induced a decrease of targeted microRNAs. BAEC cells were transfected ON with LNA directed against miR199a-3p or 199a-5p specifically (A and B). Mice were treated on three consecutive days with antagomiRs (75mg/kg/day) against miR 199a-3p/-5p and sacrificed 30 days after treatment (C and D). Results are expressed as mean ± SEM of 5 individual experiments for cells and 4 mice for *in vivo* study. *, *P.*<0.05; **, *P.*<0.01 and ***, P<0.001 *vs.* control.

Suppl fig III

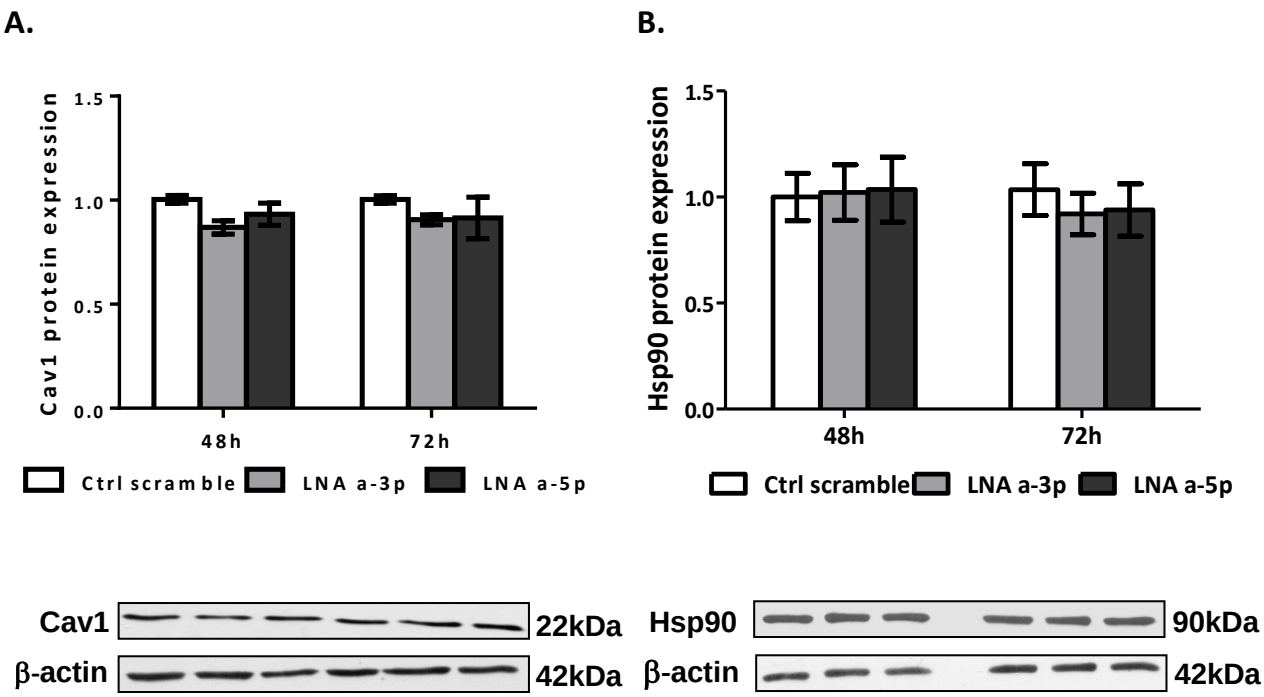

Figure III: MicroRNA 199a-3p or -5p inhibition did not induce any modification of Caveolin-1 (Cav1) and Hsp90 expression in BAEC cells. BAEC cells were transfected ON with LNA directed against miR199a-3p or 199a-5p specifically. Expression of Cav1 (A) and Hsp90 (B) were detected by Western Blotting and quantified.

Suppl fig IV

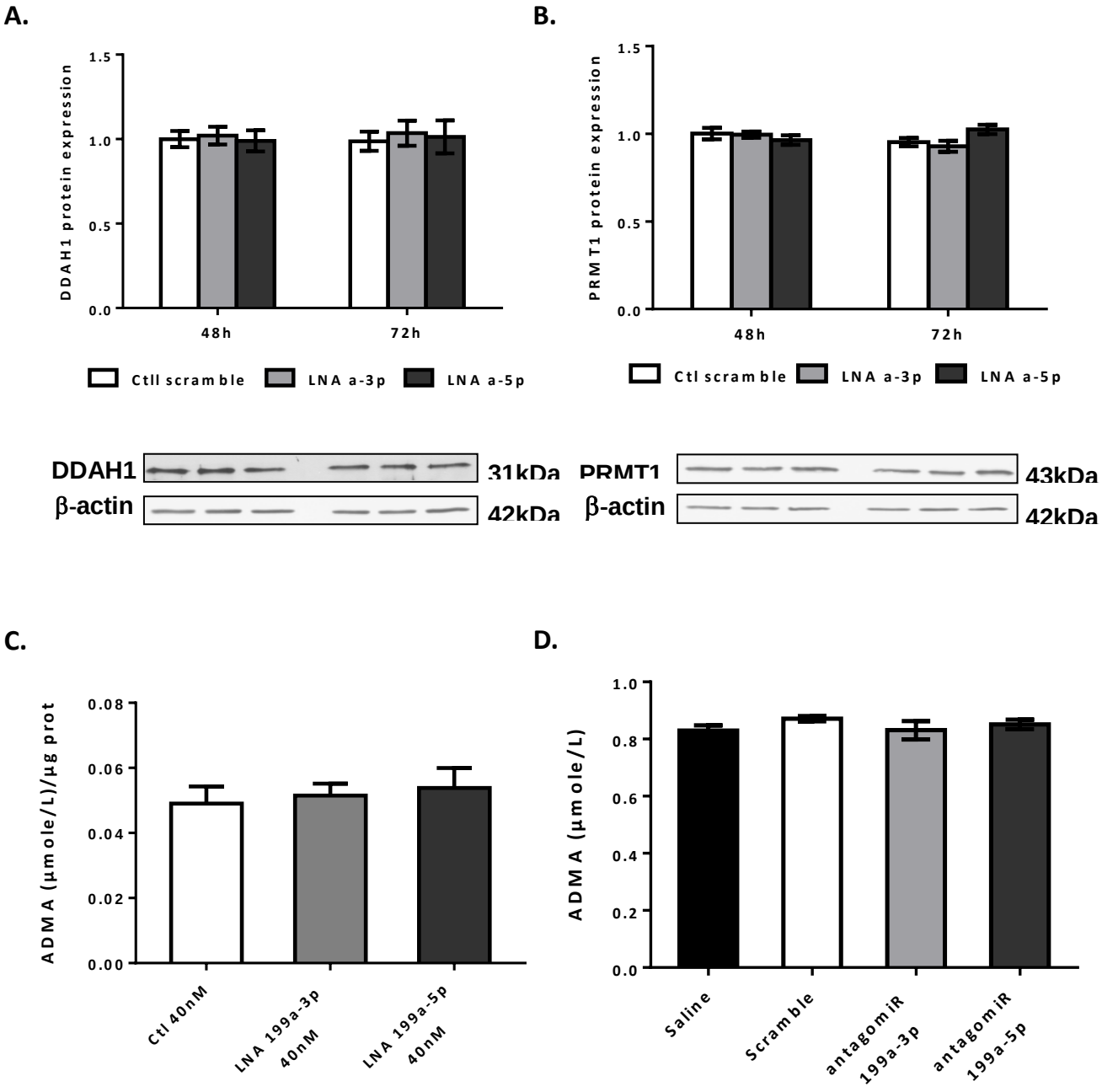

Figure IV: MicroRNA 199a-3p or -5p inhibition did not induce any modification of ADMA pathway in BAEC cells or in mice. BAEC cells were transfected ON with LNA directed against miR199a-3p or 199a-5p specifically. ADMA level was measured by ELISA quantification kit (C) and expression of PRMT1 and DDAH1 were detected by Western Blotting and quantified (A and B). Mice were treated with antagomiRs against miR 199a-3p/5p specifically, three days in a raw and sacrificed 30 days after treatment. ADMA level was measured in plasma using ELISA quantification kit (D).

Suppl fig V

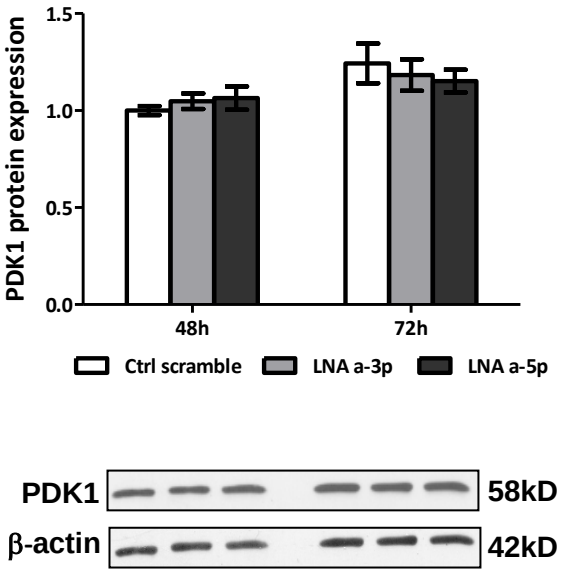

Figure V: PDK1 is not modulated by microRNAs 199a-3p/5p modulation. BAEC cells were transfected ON with LNA directed against miR199a-3p or 199a-5p specifically. Expression of PDK1 was detected by Western Blotting and quantified.

Suppl fig VI

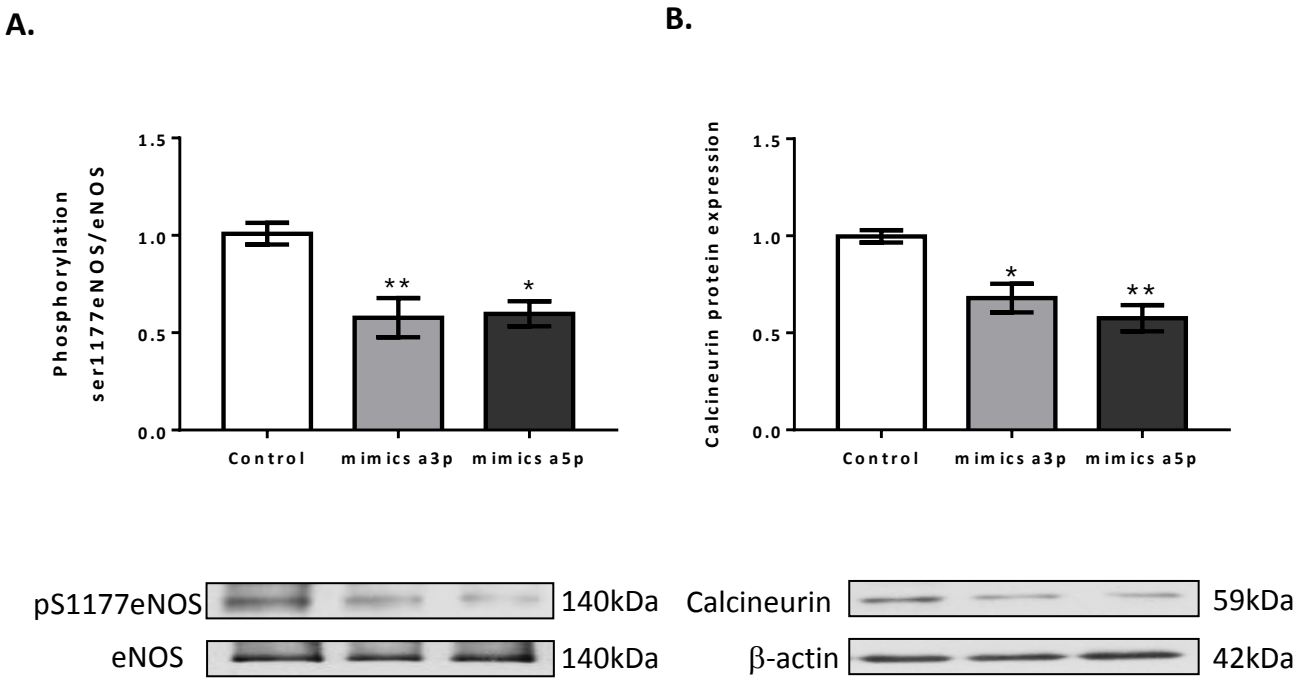

Figure VI: MicroRNA 199a-3p or -5p mimicking induces changes in serine 1177 eNOS phosphorylation and calcineurin expression. BAEC cells were transfected ON with mimics of miR199a-3p or 199a-5p specifically. eNOS phosphorylation and Calcineurin expression were detected by Western Blotting and quantified. Results are expressed as mean ± SEM of 3 individual experiments. *, *P.*<0.05 and **, *P.*<0.01 *vs.* control.

Suppl fig VII

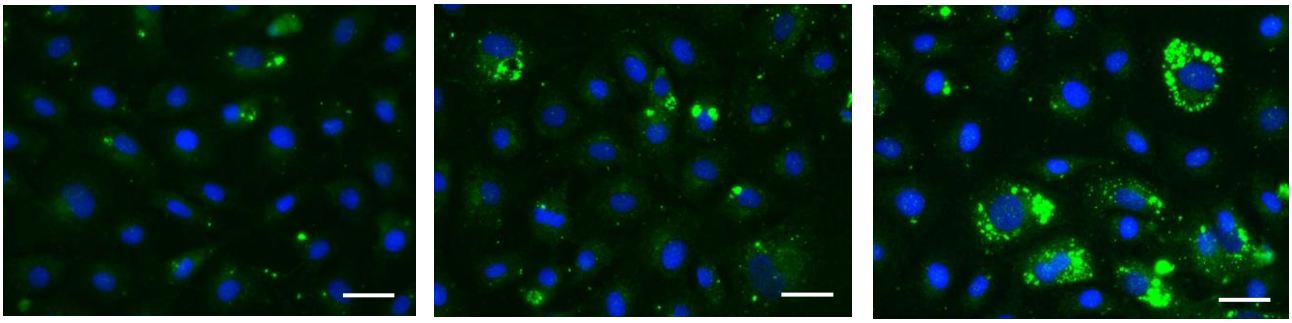

Control scramble **LNA a-3p** **LNA a-5p**

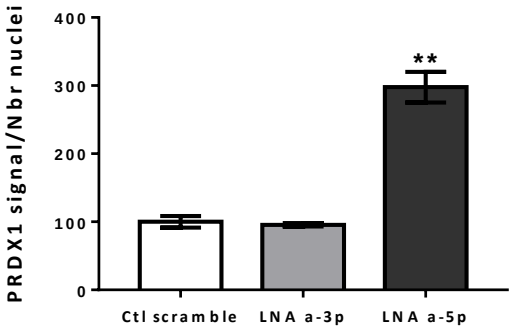

Figure VII: MicroRNA 199a-5p inhibition induced an increase of PRDX1 expression in BAEC cells. BAEC cells were cultured on glass coverslip and transfected ON with LNA directed against miR199a-3p or 199a-5p specifically. Cells were fixed with PFA 4% and incubated ON with anti-PRDX1 antibody (in green, Abcam). Nucleus were labeled using Dapi dye (blue). The signal was quantified with Image J software. Results are expressed as mean ± SEM of at least 3 individual experiments. **, *P.*<0.01 compared with control, Scale bar equals 10µm.

Suppl fig VIII

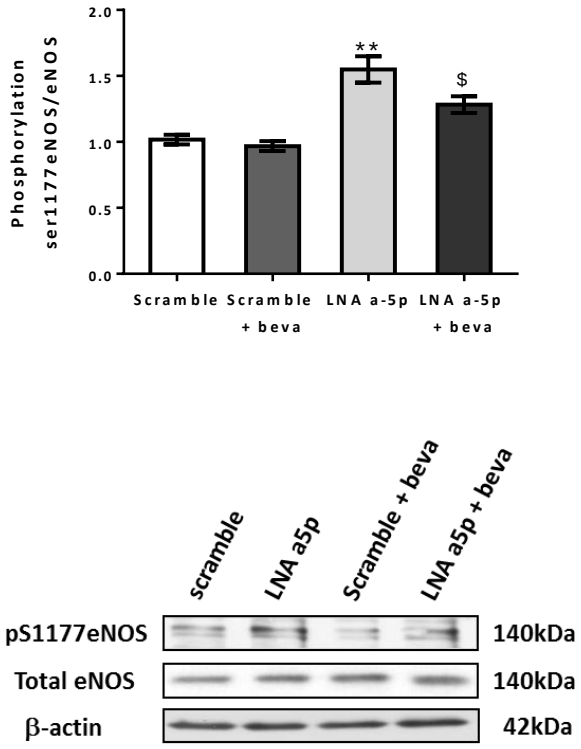

Figure VIII: Bevacizumab treatment does not induce a significant reduction of eNOS phosphorylation on serine 1177 induced by LNAa-5p. BAEC cells were transfected ON with LNA directed against miR199a-5p specifically and treated or not with bevacizumab. Phosphorylation of eNOS was detected by Western Blotting and quantified. Results are expressed as mean ± SEM of at least 3 individual experiments. **, *P.*<0.01 compared with scramble and $, P<0.05 compared with scramble + beva

Suppl fig IX

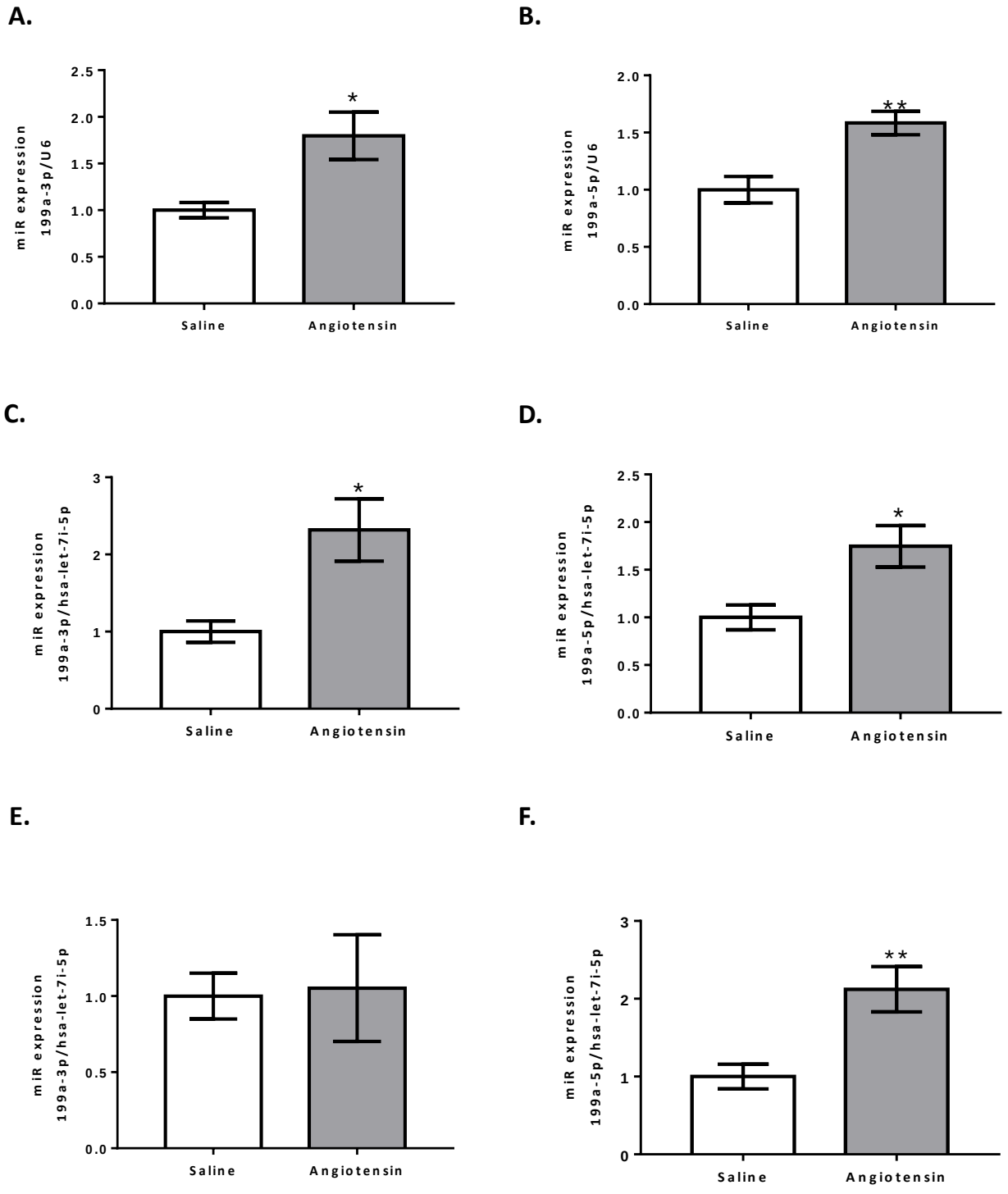

Figure IX: Hearts, vessels and plasmas isolated from mice treated with angiotensin exibit an increased microRNAs 199a expression. Mice were treated with angiotensin or saline solution during 14 days. MiR-199a-3p and miR-199a-5p were measured in hearts (A-B), aorta (C-D) and plasmas (E-F). Results are expressed as mean ± SEM of 5 animals. *, *P.*<0.05 and **, *P.*<0.01 vs. saline.